

# Interactions between Ice Sheet Dynamics and Glacial Isostatic Adjustment

The development and application of a new method to simulate the Antarctic Ice Sheet over the last glacial cycle



# Interactions between Ice Sheet Dynamics and Glacial Isostatic Adjustment

The development and application of a new method to  
simulate the Antarctic Ice Sheet over the last glacial cycle

By

C.J. van Calcar

in partial fulfilment of the requirements for the degree of

**Master of Science**

In Geoscience and Remote Sensing

at the Delft University of Technology,

to be defended publicly on Friday June 26, 2020 at 9:30 AM.

Supervisor:	Dr. W. van der Wal	TU Delft
Thesis committee:	Dr. M. Vizcaino	TU Delft
	Dr. S. l'Hermitte	TU Delft
	Dr. B. de Boer	VU Amsterdam



# Preface

The picture at the front page shows an outlet glacier at Greenwich island in the Antarctic Peninsula. The picture is taken from Prat Bay by Renato Borrás Chávez.

In the Antarctic summer of 2019, Raul Cordero and Stef l'Hermitte provided the opportunity for me to work at King George Island in the Antarctic Peninsula. It was inspiring to visit this intriguing place after following many courses about ice, snow, mass transport, oceanography, water in the atmosphere and climate change. It was at the basis on King George Island where I decided on the topic of this master thesis, with help from Wouter van der Wal. Therefore, I would like to thank Raul and Stef for giving me this opportunity.

For this thesis, I have developed a new method to study the interactions between the evolution of the Antarctic Ice Sheet and the deformation of the surface of the Earth. I have coupled two state of the art Earth and Ice models to simulate the Antarctic Ice Sheet evolution over the past 120,000 years, creating the most advanced model to study the interaction between ice and earth that is developed today. The final article, following from this thesis, will show the deformation and the change in ice thickness over the full last glacial cycle. In this thesis, I focus on the period from 120,000 to 115,000 years before present for several reasons explained in the method section.

From the moment I started this project, Wouter has surprised me over and over again with the amount of time he reserved to answer all my questions, on a daily or weekly basis, and for the very helpful discussions. Thank you very much Wouter. I would also like to thank Bas de Boer and Bas Blank for providing the models and teaching me how to work with them, and for their time to answer all my questions.

For me it feels like this thesis is the closure of a long search for a field of research that really moves me. From architecture to policy analysis to sustainable energy, I have followed courses at almost every faculty of the TU Delft. Although one of my best friends already suggested Geoscience and Remote Sensing (GRS) as a suitable study for me when I was still convinced that I would become an industrial ecologist, in 2017 I took the decision to switch studies for the last time and it was the best decision I could have taken. I finally found what I was looking for. While I was studying GRS I found out how awesome science is and how geeky I turned out to be. I even published an article about plastic transport in rivers as a first author at Environmental Research Letters thanks to Tim van Emmerik. This experience inspired and helped me to write this thesis in the form of an article.

Finally, I would like to thank my friends and family for their resoluteness to help me find a healthy balance between studying and relaxing. I would like to thank my father to always listen to me critically while I am trying to explain what I am doing and my mother for her support and for teaching me about nature, wherever we are. Last, I would like to thank Renato for his limitless faith and interest in me and for showing me the beauty of Antarctica.



# Abstract

The Antarctic ice sheet is a complex system highly influenced by global and local processes and characteristics including a varying bedrock elevation and structure of the solid Earth and a changing climate. Sea level rise has a high impact on society and the improvement of forecasts are vital to generate both adaptation and mitigation strategies. A recent comparison of 15 ice sheet models projected that the Antarctic Ice Sheet could contribute -7.8 to 30 centimeters of sea level rise between 2015 and 2100, meaning that sea level rise could increase a lot although the uncertainty is high. To better predict the future of the AIS, more accurate simulations of the evolution of the AIS are needed.

The Antarctic ice sheet consist of three main components: grounded slow-moving ice, fast flowing ice streams or outlet glaciers and floating ice shelves. Over glacial-interglacial cycles, the evolution of an ice sheet is influenced by Glacial Isostatic Adjustment (GIA) via two negative feedback loops. First, vertical bedrock deformation due to a changing ice load alters ice-sheet surface elevation. Second, bedrock deformation will change the location of the grounding line of the ice sheet. GIA is mainly determined by the viscosity of the interior of the solid Earth which is radially and laterally varying. Underneath the Antarctic Ice Sheet (AIS), there are relatively low viscosities in West Antarctica and higher viscosities in East Antarctica, which affect the response time of the above-mentioned feedbacks. However, most ice-dynamic models do not consider lateral variations of viscosity in the upper mantle in GIA feedback loops when simulating the evolution of the AIS.

The main research question of this study is:

- What is the effect of the interaction between Glacial Isostatic Adjustment and ice sheet dynamics on the Antarctic Ice Sheet growth during the last glacial cycle?

This study presents a new method to investigate 3D GIA feedback effects in detail at any chosen period during the last glacial cycle. The method is applied using ANICE and a 3D GIA FEM model. This led to the development of a fully coupled ice dynamic-3D GIA model with coupling timesteps of 1000 and 5000 years. Following the new method, the model computations alternate between the ice-sheet model, ANICE, and a 3D Finite Element Method model until convergence of the ice thickness occurs at each timestep. We simulate the evolution of the AIS from 120 000 years to 115 000 years before present, considering 1D and non-linear 3D rheologies.

The results of the coupled model are discussed in detail for the period 120,000 years to 115,000 years before present with a focus on the Siple Coast and the Ross Ice Shelf. The maximum difference between the uncoupled deformation (iteration 1) and the coupled deformation (average between the last two iterations) for the period 120,000 to 115,000 years BP is 3 to 8 mm per year, depending on the viscosity of the upper mantle. The maximum difference in ice thickness at 115,000 years BP is 50 meters close the Ronne Ice Shelf and the Ross Ice Shelf. The grounding line position differs up to 80 meters when applying the coupling method compared to the uncoupled result.

The increases in deformation using a 3D wet rheology with a grain size of 10 mm are highest at the Siple Coast, the Ronne Ice Shelf, and several other locations along the grounding line of the AIS. The results of this study emphasize the importance of the 3D GIA feedback effects when simulating the evolution of the AIS during the last glacial cycle. Therefore, the GIA feedback effects should be taken into account in future studies.





# Contents

<b>Preface</b> .....	<b>v</b>
<b>Abstract</b> .....	<b>vii</b>
<b>Contents</b> .....	<b>ix</b>
<b>List of Abbreviations</b> .....	<b>xi</b>
<b>List of Figures</b> .....	<b>xii</b>
<b>1 Introduction</b> .....	<b>15</b>
1.1 Antarctica .....	16
1.1.1 From emergence to present day .....	16
1.1.2 Measuring and simulating .....	16
1.1.3 The impact of the Antarctic Ice Sheet .....	17
1.2 Dynamics of the Antarctic Ice Sheet and the solid Earth .....	18
1.2.1 Ice dynamics.....	18
1.2.2 Glacial Isostatic Adjustment.....	19
1.2.3 Interaction between ice load and deformation.....	20
1.3 Numerical modelling of GIA feedback effects .....	22
1.3.1 GIA models.....	22
1.3.2 Coupling of a GIA model and an ice model.....	23
1.4 Research objective and questions.....	24
<b>2 Article</b> .....	<b>27</b>
<b>3 Conclusions</b> .....	<b>53</b>
<b>A Ice dynamic model</b> .....	<b>57</b>
A.1 Forcing.....	57
A.2 Including the calculated GIA file in ANICE .....	58
<b>B GIA model</b> .....	<b>59</b>
B.1 Generation of a layered model.....	59
B.2 Input: define ice and ocean loads.....	61
B.3 Running the FEM model .....	61
<b>C Interpolation between model grids</b> .....	<b>63</b>
C.1 Interpolation ANICE to FEM.....	63
C.2 Interpolation FEM to ANICE.....	65
<b>D Method</b> .....	<b>69</b>

D.1 Conversion of the model.....	69
D.2 Recommendations for model improvement.....	70

# List of Abbreviations

<b>AIS</b>	Antarctic Ice Sheet
<b>FEM</b>	Finite Element Method
<b>FVM</b>	Finite Volume Method
<b>GIA</b>	Glacial Isostatic Adjustment
<b>GPS</b>	Global Positioning System
<b>LGM</b>	Last Glacial Maximum
<b>PD</b>	Present Day
<b>SIA</b>	Shallow Ice Approximation
<b>SSA</b>	Shallow Shelf Approximation
<b>WAIS</b>	West Antarctic Ice Sheet
<b>ELRA</b>	Elastic Lithosphere Relaxing Asthenosphere

# List of Figures

1.1	Southern Ocean bathymetry, regional seas, and ice shelves. Red markers indicate permanently occupied Antarctic Stations, blue markers indicate seasonally occupied stations. Ice shelves: 1, Filchner; 2, Riiser-Larsen; 3, Fimbul; 4, West; 5, Shackleton; 6, Getz; 7, Abbott; 8, George VI; and 9, Wilkins. Image taken from Stark et al. (2019)...	15
1.2	Velocities of the Antarctic ice sheet measure with remote sensing. Figure taken from Mouginot et al.,(2017).....	18
1.3	Schematic Figure of the ice melting process and grounding line retreat for a retrograde slope (Figure A) and a prograde slope (Figure B). Figure taken from Pattyn and Morlighem (2020).....	19
1.4	The stabilizing effect of GIA feedbacks. a) The equilibrium situation where the ice sheet is not gaining or losing mass, where $h_1$ is the ice thickness and $d_1$ is the sea level at the position of the grounding line. The ice flux, $q_1$ , is a function of the ice thickness. b) The top of the ice sheet melts, leading to a thinner ice shelf and grounding line retreat. c) The situation after the GIA feedback. Figure taken from Whitehouse et al. (2019).....	21
1.	Schematic overview of the developed forward coupling method. It is shown that several iterations occur within one timestep until the convergence criterium of a maximum difference of 10 meter of deformation has been met for all elements of the GIA model. ....	33
2.	Differences between 1D and 3D rheologies of which the viscosity is shown in Figures A-C at a depth of 246 kilometers. Figure A corresponds to the 1D rheology. The blue ellipse encircles the Siple Coast. Figure B corresponds to a dry rheology with a grain size of 4 mm. Figure C corresponds to a wet rheology with a grain size of 10 mm.....	35
3.	Mean deformation rate over a certain timestep. Figure A shows the mean deformation rate over the period 20,000 years to 19,000 before present. Figure B shows the mean deformation rate over the last 1000 years until modern date. Note that the scales are different. ....	36
4.	Figures A-C show the deformation of the Earth's surface when applying the same load using the 3 different rheologies at the first timestep from 120,000 years to 115,000 years before present. Figure B and C show the difference with Figure A. The grounding line is shown with the black line. Figures D-F show the effect of the change in deformation on ice thickness where Figures E and F show the difference between the 3D simulation and the 1D simulation. The green and orange line correspond to the grounding and calving line, respectively. A yellow grounding line and a black calving line are shown in Figures E and F at locations and correspond to the line resulting from the 3D rheology. Note that the black and yellow line are only visible around the Ronne Ice Shelf and the Ross Ice Shelf.....	37

5.	Close up at grounding line migration differences between the 1D simulation and the 3D simulations. Figure A shows the difference in grounding line migration and ice thickness between the 1D simulation and the 3D dry simulation. Figure B shows the difference in grounding line migration and ice thickness between the 1D simulation and the 3D wet simulation. ....	38
6.	Iterative process of timestep 1, 120,000 to 115,000 years BP, using the wet 3D rheology with a grainsize of 10 mm. Figures A-D show the ice thickness at 115,000 years BP where Figures B and C show the difference ice thickness of the corresponding iteration with the iteration before. Figures E-H show the deformation rate when applying the load shown in Figures A-C, where Figures F and G show the deformation difference of the corresponding iteration with the iteration before.....	36
7.	A) Accumulated convergence uncertainty at Last Glacial Maximum B) Added convergence uncertainty during the period 20 000 years BP to modern date. C) Accumulated convergence uncertainty at modern date.....	39
S.1	Atmospheric temperature (black) and eustatic sea level relative to present day (red). Both are shown over time, starting 120 000 years BP.....	49
S.2	Overview of the iterative process of the coupling method for timestep 5; 95 000 till 90 000 years ago. Antarctica is shown on a equidistant, Asia centred, grid at all longitudes. The black line is the grounding line at 90 000 years ago of iteration 3 and is the same in every Figure to allow for comparison. A) Relative sea level and ice thickness in meters multiplied by the assumed density of water and ice respectively computed by ANICE. The difference is shown between the final load at step 4 and the first iteration of step 5. The input for iteration 0 is the final deformation of step 4. B) Computed deformation by the GIA model using the load from Figure A as input. The difference is shown between iteration 0 of step 5 and the final deformation of step. This shows the effect of the change in load shown in Figure A. C-G) Difference in load and deformation with former iteration. G) Addition of figures D and F. H-I) Difference in load and deformation with former iteration. J) Addition of figures F and I. The difference is everywhere smaller than 10 meters and the convergence criterium has been met. K) Difference between final load of step 5 and the load from iteration 0. The final load of step 5 is calculated by taking the mean value at each grid cell from iterations 2 and 3. L) Difference of final deformation between timestep 4 and 5. The final load of step 5 is computed by ANICE using the final deformation of step 5 as input. Figures K and L show the total effect of the full iteration process.....	49
S.3	The assumed change in ice and ocean load for the period 120,000 years BP to 115,000 years BP, following from a deformation that is close to zero.....	50
s.4	Iteration process of timestep 1, 120,000 to 115,000 years BP, using three different rheologies. For the three different rheologies, the same initial load is applied at iteration 1. Figures A-C show the deformation rate for the 1D rheology, where figures B and C show the difference in deformation of the mean of the last two iterations with iteration 1. Figures D-G show the deformation rate for the 3D dry rheology with a grain size of 4 mm. Figures H-K show the deformation rate for the 3D wet rheology with a grain size of 10 mm.....	50

S.4	Iteration process of timestep 1, 120,000 to 115,000 years BP, using three different rheologies. For the three different rheologies, the obtained deformation from Figure S.3 is used at iteration 1. Figures A-C show the ice thickness for the 1D rheology, where figures B and C show the difference in ice thickness of that iteration with iteration 1. Figures D-G show the ice thickness for the 3D dry rheology with a grain size of 4 mm. Figures H-K show ice thickness for the 3D wet rheology with a grain size of 10 mm.....	51
B.1	Difference between finite volume approach and finite element approach (Latychev et al., 2005).....	59
C.1	Ice thickness at Antarctica. Output from the ANICE model at a polar centered grid....	64
C.2	Ice thickness at all longitudes and latitudes at a resolution of a quarter of a degree, linearly interpolated.....	64
C.3	Ice thickness at all longitudes and latitudes at a resolution of a quarter of a degree, interpolated using Greens method. No plane tension is apparent, sinusoide are visible.....	65
C.4	Ice thickness at all longitudes and latitudes at a resolution of a quarter of a degree, interpolated using quadrant method.....	65
C.5	Deformation of the Earth's surface from 120 000 till 20 000 years before present.....	66
C.6	Deformation of Antarctica interpolated to a polar centered grid using the linear method.....	66
C.7	Deformation of Antarctica interpolated to a polar centered grid using the radius method.....	67

## Introduction

Antarctica is a continent of approximately 14 million square kilometers lying at the south pole of planet Earth and is circled by the Southern Ocean. Atmospheric temperatures can go down to -90 degrees Celsius. The ocean has the strongest current in the world (Bell & Seroussi, 2020) and plays an important role in the global climate system (Stark et al., 2019). An immense ice sheet rests on the continent, which is currently the driest desert in the world. At some places in East Antarctica, the ice thickness grew up to 5 kilometers during the last glacial cycle. The melting of the full ice sheet would account for approximately 58 meters of mean global sea level rise (Morlighem et al., 2020). There is a mountain range separating East and West Antarctica and there are multiple lakes hidden under the ice (Creys et al., 2014). The current shape of the continent, including the names of many floating ice shelves and the seas around the continent, is shown in Figure 1.1. Although this remote continent inhabits only a thousand people, it is home to many species of penguins, birds, seals, fish, and crustaceans that have adapted to this extreme environment.

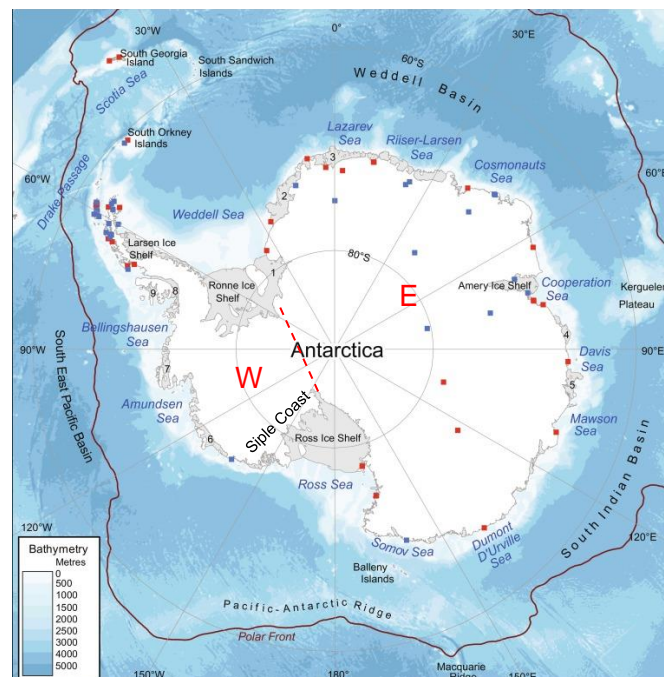


Figure 1.1: Southern Ocean bathymetry, regional seas, and ice shelves. Red squared markers indicate permanently occupied Antarctic Stations, blue squared markers indicate seasonally occupied stations. Ice shelves: 1, Filchner; 2, Riiser-Larsen; 3, Fimbul; 4, West; 5, Shackleton; 6, Getz; 7, Abbott; 8, George VI; and 9, Wilkins. Figure after Stark et al. (2019).

Section 1 provides the basic knowledge needed to understand why this study is important (subsection 1.1), the history and current state of the Antarctic Ice Sheet (subsection 1.2) and the dynamics of the Antarctic Ice Sheet and the solid Earth (subsection 1.3). Background information about ice dynamic models and GIA models is provided in subsection 1.4. The research questions of this study and the outline of the report are presented in subsection 1.5.

## 1.1 Antarctica

### 1.1.1 From emergence to present day

The Antarctic continent became tectonically isolated and found its place where it is now about 100 million years ago (Barret, 1996). From seismic data it is known that the crust at East Antarctica was still relatively thin and the upper mantle had a relatively low viscosity compared to present day. Nowadays, the structure of the Earth's mantle is very different between West Antarctica and East Antarctica, where the crust is thicker and the viscosity higher (Heeszel et al., 2016). The bedrock topography of Antarctica is continuously changing due to erosion, sedimentation, and tectonic activity (Whitehouse et al., 2019).

The first ice formations started 34 million years ago on high elevations due to a cooling climate forced by a drop of global atmosphere and ocean temperatures and a drop of CO<sub>2</sub> concentrations in the atmosphere (Bell & Seroussi, 2020). For the next 20 million years, East Antarctica remained glaciated, but the ice sheet has been growing and melting caused by changing climate conditions and changes in the Earth's orbit around the sun. Changing climate conditions arose naturally due to feedback loops. The albedo of the Earth represents its reflectivity. An increasing ice sheet area leads to a higher albedo and consequently to a cooler climate. On the other hand, more ice cover and reduction of precipitation during glacials reduces the amount of flora and the uptake of CO<sub>2</sub>. An increased concentration CO<sub>2</sub> in the atmosphere leads to the enhancement of the greenhouse effect (Meredith et al., 2019).

Between 14 and 10 million years ago, the climate cooled down even further and the bedrock experienced high uplift rates due to tectonic movements. Consequently, the West Antarctic ice sheet (WAIS) began to grow on what was first a shallow sea (Bell & Seroussi, 2020). During some warm periods, the WAIS retreated beyond its current extent and in some instances completely collapsed (Naish et al., 2009). From 10 million years ago, glacial and interglacial periods were mostly forced by insolation cycles as the result of a changing orbit of the Earth around the sun (Petit et al., 1999). The last glaciation period, starting around 120,000 years before present (BP), had a fast growth of ice at the start and stabilizes closer towards the Last Glacial Maximum (LGM) between 21 to 27 thousand years BP. From LGM till present day, the ice sheet has been decaying.

### 1.1.2 Measuring and simulating

To study Antarctica, the research stations shown in Figure 1.1 are built as a basis from which all types of measurements are performed, such as seismicity, gravimetry, photogrammetry, ice core boring and many more. These measurements provide data to study the current state of Antarctica, and in some cases to study the history of Antarctica. The long-term evolution of the Antarctica Ice Sheet (AIS) can be simulated by using ice dynamic models. Ice core and sediment analyses provide information that can be used to validate the models.

One of the tools to compute recent changes of ice mass and ice sheet surface elevation is remote sensing data from satellites. Global Positioning System (GPS) measurements can be used to measure surface elevation of the ice sheet and satellite gravimetry observations can be used to measure changes in ice mass. However, these measurements are influenced by deformation of the Earth's surface. For example, GPS measurements show an uplift rate of the Earth's surface at the Amundsen Sea Embayment of 4 centimeters per year (Barletta, 2018). The uplift is composed of a response of the elastic crust of the Earth to recent ice mass loss and a response of the visco-



elastic mantle of the Earth to recent and historic ice mass loss. The deformation of the Earth's interior in response to changes in ice and ocean loading is called Glacial Isostatic Adjustment (GIA). To compute changes in the ice thickness, the measurements of ice sheet elevation should be corrected for GIA. Even more important is the correction for ongoing solid Earth deformation of satellite gravimetry observations to compute present day changes of mass.

Several models are developed to simulate recent and historical deformation rates. Because remote sensing data are only available since 40 years and not all parameters of ice mass change can be measured, a combination of remote sensing data and models is required to compute the ice sheet evolution and to determine current rates of ice mass change.

### 1.1.3 The impact of the Antarctic Ice Sheet

The AIS is an important part of the climate system of the Earth and acts as a thermostat (Meredith et al., 2019). Incoming solar radiation is reflected to space due to the high albedo of the surface of the ice sheet. On the other hand, the ice sheet protects the atmosphere from radiation from the Earth and therefore prevents warming of the atmosphere. This way, the melting of the AIS affects the global climate, and therefore also the glaciers worldwide and the Greenland ice sheet.

Observations from satellite measurements show several regions of Antarctica where ice mass decays and where outlet glaciers are retreating and flowing faster where ice is exposed to warm ocean waters (Shepherd et al., 2018). The time frame of natural melting and growing processes is 40,000 to millions of years. Consequently, the typical ice melt and growth rates forced by natural processes are several millimeters year. However, satellite data gathered in the last two decades show more rapid ice mass change of -10 meter/year in West antarctica and +0.5 meter per year in East Antarctica and the Ross sea embayment (Smith et al., 2020). The estimated ice mass loss between 1992 and 2017 is  $2.7 \pm 1.4$  billion tons of ice, corresponding to a contribution to sea level rise of  $7.6 \pm 3.9$  millimeters (Shepherd et al., 2018).

Due to the shape of the bedrock topography and the big volume of ice shelves floating on ocean water, Antarctica could be highly vulnerable to projected increases in ocean temperatures (Turney et al., 2020). A recent comparison of 15 ice sheet models projected that the Antarctic Ice Sheet (AIS) could contribute -7.8 to 30 centimeters of sea level rise between 2015 and 2100, meaning that sea level rise could increase a lot although the uncertainty is high (Seroussi et al., 2020).

A changing climate and sea level have a large impact on all living beings worldwide. The flora and fauna at Antarctica are facing locally and globally induced anthropogenic climate change (Chown & Brooks, 2019). An increasing sea surface temperature and changing wind direction and strength has a broad influence on ecosystems and aspects of the biology of animals, including their breeding phenology, foraging success, survival, and reproductive performance (Constable et al., 2014). For example, Antarctic marine mammals are dependent on krill as their main source of food. As sea temperature is rising and sea ice is decreasing, the krill stock also decreases (Atkinson, 2004). An increasing accuracy of ice sheet evolution projections lead to more accurate predictions of the effect of climate change on life.

Sea level rise puts pressure on coastlines and cause cities at coastlines around the world to subside (Muis et al., 2020; Oppenheimer et al., 2019). This has a high impact on society and the improvement of sea level change forecasts are vital for adaption of protective initiatives against sea level rise. These forecasts can help policymakers to decide on what investments should be done to protect both people and the environment.

To be able to forecast future sea level change, it is necessary to understand how the AIS responds to a changing climate and how the Earth responds to a changing ice and ocean load. This knowledge is gained by using ice sheet evolution models that simulate the history of the AIS and GIA models that simulate the Earth's response to loading. Thus, to improve sea level change projections, accurate simulations of the history of the AIS are needed. This thesis discusses the

ice dynamics of the Antarctic ice sheet, the resulting bedrock deformation, and a new method to simulate the interaction between these processes.

## 1.2 Dynamics of the Antarctic Ice Sheet and the solid Earth

### 1.2.1 Ice dynamics

The Antarctic ice sheet consists of three main components: grounded slow-moving ice, fast flowing ice streams or outlet glaciers and floating ice shelves. East Antarctica mainly consists of grounded slow-moving ice. Recent remote sensing measurements indicate low velocities of 1 meter per year for grounded ice, compared to velocities of 4 kilometers per year of ice streams and outlet glaciers (see Figure 1.2) (Mouginot et al., 2017).

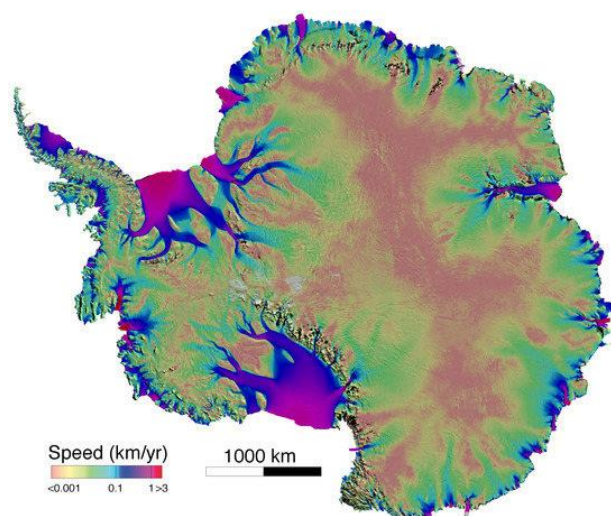


Figure 1.2: Horizontal velocities of the Antarctic ice sheet measured with remote sensing. Figure taken from Mouginot et al. (2017).

The climate and sea level are the main factors causing the ice sheet to grow or decay. The ice sheet gains mass through snowfall at its surface and loses mass primarily by melting beneath its floating ice shelves and by calving icebergs, but also by surface melt driven by solar radiation. When grounded ice thickness increases, a flow towards the outer parts of the ice sheet is created. This flow brings ice formed at the ice sheet towards floating ice shelves. In return, the ice shelves exert a resistive stress on the grounded ice called buttressing (Goldberg et al., 2009). Buttressing, together with a high horizontal speed of ice shelves up to 3 kilometers per year, play a key role in ice dynamics (Mouginot et al., 2017; Gagliardini et al., 2010).

The line where grounded ice is no longer connected to the bedrock and becomes floating ice, is called the grounding line. Circumpolar deep water of 4 degrees Celsius reach grounded ice at the grounding line and melts the ice shelf from below (Pattyn & Morlighem, 2020). Due to melt from below, the ice shelf thins and at some point, the outer parts break into icebergs. The line where ice shelves break into icebergs is called the calving line.

Relatively warm circumpolar deep water not only causes the ice shelf to thinner, it also causes the grounding line to retreat. Since the topography of Antarctica lies partly below current sea level, and some regions have a downward going bedrock slope when going inland, the grounding line retreat continues, and the ice sheet becomes unstable (Schoof, 2007). This is known as the Marine Ice Sheet Instability (MISI) and is shown in Figure 1.3A. A few places exist, such as the Crane Glacier in the Antarctic Peninsula, where the ocean and the atmosphere are warming quickly enough to melt the ice shelf quicker than the seaward flow. If reverse-sloping bedrock is more than 1000-meter-deep, grounding line cliffs that are not being covered by ice shelves could break and form icebergs (DeConto & Pollard, 2016). This is known as the Marine Ice Cliff

Instability (MICI) and is shown in Figure 1.3B. An unstable ice sheet could lead to the Antarctic collapse where grounded ice continuously melts fast due to the disappearance of ice shelves and consequently the lack of buttressing (DeConto & Pollard, 2016).

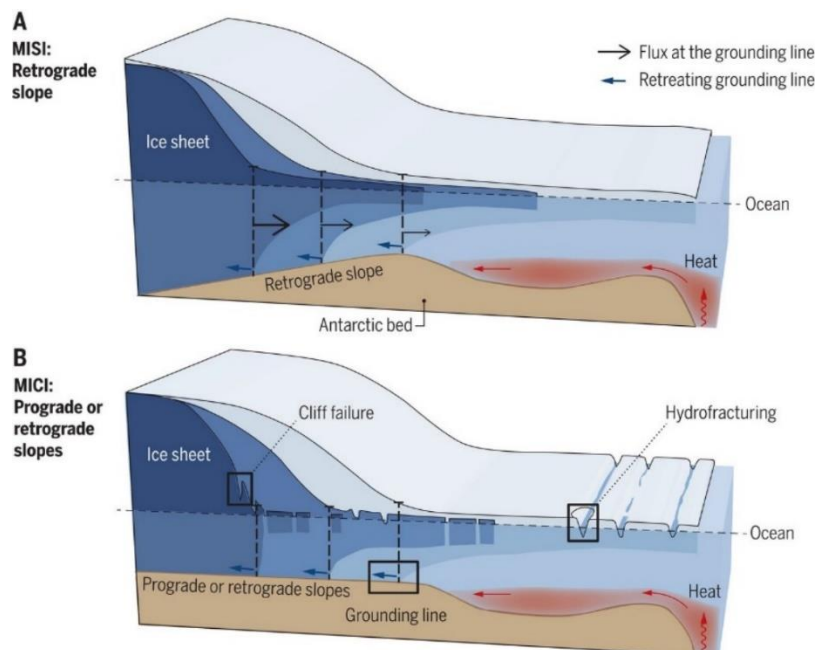


Figure 1.3: Schematic Figure of the ice melting process and grounding line retreat for a retrograde slope (Figure A) and a prograde slope (Figure B). Figure taken from Pattyn and Morlighem (2020).

### 1.2.2 Glacial Isostatic Adjustment

Besides climate and sea level as the main factor that causes the ice sheet to grow or decay, the evolution of the ice sheet also depends on the response of the Earth to changes in the thickness of the ice sheet. As explained in section 1.1.2, the interior of the Earth partly consists of viscoelastic material and deforms over time due to loading, called GIA. The Earth acts elastic on short time scales and viscous over long time scales. The load of the ice sheet pushes the Earth's surface down. The material under the ice sheet subside and moves outwards towards the margins of the ice sheet, causing an uplift of the Earth's surface around the ice sheet, called the forebulge. The load on the Earth's surface causes radial and, in lesser extent, lateral movements of the material.

The solid Earth can be divided into approximately six layers based on material properties. From the center of the Earth to the Earth's surface: the inner core, outer core, lower mantle, asthenosphere, upper mantle, and crust. The upper mantle and the crust together are called the lithosphere, which is the rigid layer on top of the more ductile viscoelastic asthenosphere. The lower mantle behaves elastic as well as viscoelastic. The outer core is fluid and the inner core is solid.

The core provides a buoyancy force to the lower mantle. The upper mantle gives an upward force towards the crust, which floats on the mantle at an elevation that depends on its thickness and density. If the load is low, elastic crust will still react, but the viscoelastic mantle will not change much. When load is removed due to melting of the ice sheet or a decrease in sea level, material in previously ice-covered areas rises until the crust and the upper mantle are in isostatic equilibrium. The isostasy of the buoyancy of the crust (floating on the mantle) depends on the crust's density and thickness. It takes ten thousands of years to reach isostatic equilibrium after a glaciation period. Since the load is changing on shorter timescales, this equilibrium is never

reached. Therefore, today's observed deformation is the result of multiple glacial loading cycles (Whitehouse, 2009).

Deformation is controlled by two components. First, the thickness of the lithosphere influences the wavelength of deformation. Second, the viscosity of the mantle controls the rate of deformation. Subduction of oceanic plates transports water into the upper mantle. The material in the upper mantle is olivine and controls the viscosity, as well as the temperature profile of the mantle and water content in the upper mantle (Karato, 1986). A temperature profile can be made based on seismic models. Seismic wave speed relates to temperature distribution in the mantle and that relates to mantle viscosity.

The Earth is not only radially varying but also laterally. Low viscosity regions are likely to occur at active plate boundaries (Alaska, Iceland, Northern Antarctic Peninsula, Patagonia) because of the high mantle temperatures. Here, viscous deformation will be dominated by the response to recent ice mass change. To correct satellite observations for ongoing GIA, it is often assumed that GIA is linear in time and reflects the viscous response to long-past ice sheet change and any non-linear effect reflects the elastic response to contemporary ice-sheet change. However, the bedrock deformation has a short relaxation time in low-viscosity regions so the response may not be linear over the period of geodetic measurements. Recent deformation rates may therefore contain both elastic and viscous signals.

Nield et al., (2014) showed this effect in the Antarctic peninsula where the bedrock uplift is the viscoelastic response of the Earth caused by recent ice unloading. The viscosity of the lithosphere is much lower in West Antarctica than in East Antarctica due to a difference in temperatures of the mantle, in water content and in grain size (Nield et al., 2018; Heeszel et al., 2016). Recent studies estimate the viscosity of the upper mantle under certain regions in West Antarctica, for example Amundsen Sea Embayment, to be two orders of magnitude lower than previously assumed (Barletta et al., 2018; Wolstencroft et al., 2015). The presence of such low mantle viscosities has effects on the millennial time scale and has important implications on collapse scenarios of West Antarctica and on the development of ice sheet evolution models and GIA models (Barletta et al., 2018).

### 1.2.3 Interaction between ice load and deformation

The interaction between the vertical deformation of the Earth's surface and a changing ice load is referred to as GIA feedback effects. The interaction occurs in two ways. First, the load of the ice sheet causes downward vertical deformation of the Earth's surface, leading to a lower elevation of the ice sheet surface. Precipitation patterns are different at different elevation and the atmospheric temperature increases at lower elevations. As a result, the ice mass loss or gain at the top of the ice sheet surface changes. A change in ice mass will lead to a change in deformation of the Earth's surface. On its turn, deformation affects the ice mass change again. This is called a GIA feedback loop.

Second, deformation of the Earth's surface not only affects the surface elevation of the ice sheet directly, but also the sea level. Figure 1.4a shows the ice sheet and the ice shelf in equilibrium, where  $h_1$  is the thickness of the ice and  $d_1$  is the sea level at the position of the grounding line. A thinner ice sheet thickness as a result of surface melt leads to an increased ice flux towards the ice shelf (shown in Figure 1.4b). The thickness is proportional to the water depth, resulting in a large reduction in grounded ice caused by a small increase in water depth at the grounding line (Whitehouse et al., 2019). On its turn, a reduction in grounded ice leads to upward deformation of the Earth's surface and the local sea level lowers due to the diminishing gravitational attraction of the ice on the surrounding water (de Boer et al., 2017). The local shallowing of water reduces the loss of ice across the grounding line (shown in Figure 1.4c).

The effect of the GIA feedback on the grounding line migration is dependent on the deformation rate, the bedrock slope, and ongoing viscous uplift of the Earth's surface

(Whitehouse et al., 2019). A lower sea level, because of the GIA feedback, reduces the ice loss around the grounding line. Therefore, the GIA feedback effect stabilizes, and in some cases halting, migration of the grounding line along reversed bed slopes (Larour et al., 2019; Gomez et al., 2012). Ongoing viscous uplift of the bedrock could even initiate a readvance of the grounding line (Pollard et al., 2017).

Since bedrock deformation rates are highly dependent on the viscosity of the interior of the Earth, also the GIA feedback effect is dependent on the viscosity. The stabilizing GIA feedback effect is quick at regions containing relatively low mantle viscosities because the mantle approaches isostatic equilibrium 1-2 orders of magnitude faster compared with global-average timescales, resulting in high deformation rates (Whitehouse et al., 2019). The GIA feedback effects play an important role in regional ice sheet evolution of the AIS because of the strong relation with the viscosity of the Earth (Larour et al., 2019; Whitehouse et al., 2019; Pollard et al., 2017;).

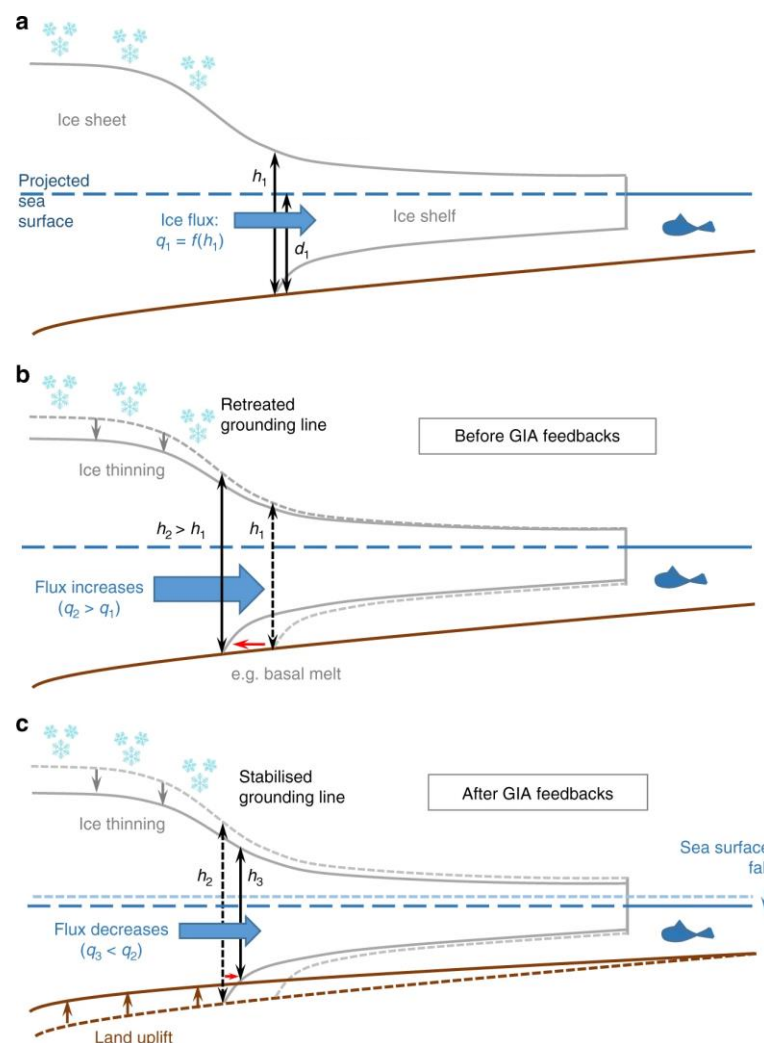


Figure 1.4: The stabilizing effect of GIA feedbacks. a) The equilibrium situation where the ice sheet is not gaining or losing mass, where  $h_1$  is the ice thickness and  $d_1$  is the sea level at the position of the grounding line. The ice flux,  $q_1$ , is a function of the ice thickness. b) The top of the ice sheet melts, leading to a thinner ice shelf and grounding line retreat. c) The situation after the GIA feedback. Figure taken from Whitehouse et al. (2019).

## 1.3 Numerical modelling of GIA feedback effects

### 1.3.1 GIA models

GIA can be simulated by calculating the response of a model of the Earth by applying a certain load. A GIA model computes the stress within the Earth model over long timescales of ten thousands to hundred thousands of years by using the ice load history results from ice dynamic models. The level of detail in terms of, among others, radial and lateral resolution and material properties of the model of the Earth differs per model and is dependent on the goal of the study, the available computational power and the available resources to develop a GIA model. The calculation of laterally and radially varying deformation over time is a computationally expensive model and takes a long time to finish a simulation. Therefore, deformation is often simulated with GIA models that do not include a laterally varying Earth structure, called 1D GIA models. GIA can be included in several ways in an ice dynamic model, which are discussed in this section.

For example, the bedrock response to load can be calculated using an Elastic Lithosphere Relaxing Asthenosphere (ELRA) model (Le Meur & Huybrechts, 1996). This is a two-layer model that contains a local elastic lithosphere and a relaxing asthenosphere using a constant relaxation time. The elastic lithosphere is modelled as a thin plate with flexural rigidity that deforms linearly. The relaxing asthenosphere is simulated more accurately by using the diffusion equation for mantle movement. The ELRA model is effective in computing the bedrock response and therefore favorable to compute the evolution of an ice sheet on long timescales.

Radially varying self-gravitating visco-elastic spherical Earth models compute the complete Earth composition with an inviscid core, viscoelastic lower and upper mantle and elastic lithosphere, accounting for gravity field perturbations and displacements using spherical harmonics (De Boer et al., 2014; Le Meur and Huybrechts, 1996). When a load is placed on a visco-elastic body, the body deforms by stress and strain, which are dependent on the viscosity of the mantle and the elastic parameters of the crust, such as density and rigidity. Rheological models are used to describe the relation between stress and strain.

There are different ways to calculate the spatially time-dependent response of the Earth to surface load. For example, the Maxwell rheology and the Burgers rheology assume the Earth is a linear viscoelastic body. The response can be calculated using viscoelastic Love numbers. These Love numbers reflect the assumed viscosity profile of the mantle.

Non-linear stress-strain relationships form the basis of the power-law approach (Wu, 1998). The power-law approach assumes the Earth is a nonlinear viscoelastic body where the effective viscosity depends on the stress field throughout the mantle, which depends on the surface load change and on internal changes due to mantle convection. The effective viscosity can be described by diffusion creep and dislocation creep that can be derived from seismic models. Diffusion creep is linearly dependent on stress caused by pressure and largely dependent on grain size (the material of the asthenosphere consists of grains). Various vacancies exist within the crystal lattice. Given a certain stress, the vacancies migrate from their sources to vacancy sinks (Gordon, 1965). At lower temperatures, grain boundary diffusion allows for mass transport along the grain boundaries themselves (Ranally, 1995).

Dislocation creep is the main process of material movement when the applied load is high and is mainly dependent on the water content (Ranally, 1995). Dislocation creep is linearly dependent on grain size and nonlinearly dependent on stress due to the time dependent effective viscosity (Hirth & Kohlstedt, 2003). The relation between stress and diffusion and dislocation creep is dependent on grain size, water content, melt content and temperature.

### 1.3.2 Coupling of a GIA model and an ice model

The GIA feedback effects can be simulated using a coupled ice dynamic - sea level model by incorporating the gravitationally self-consistent sea level equation (de Boer et al., 2014). The sea level model computes the bedrock deformation and the relative sea level change and forwards this to the ice sheet model. The ice sheet model uses the bedrock deformation to determine the change in topography. This adjusted topography is used to compute the ice sheet evolution.

Currently used sea level models do not account for laterally varying mantle viscosities. It is shown that ice thickness varies when more sophisticated GIA models are used due to a highly varying viscosity in the mantle under Antarctica (Heeszel et al., 2016; Nield et al., 2018). There are different ways to model a laterally varying Earth structure. For example, Oude Egbrink (2017) divided Antarctica in different regions based on the viscosity of the mantle. Here, locations with similar mantle viscosities will form 1 region. The average viscosity per region is transformed to relaxation times, which can be used by the ice model to determine the new topography.

Another way of including the laterally varying Earth structure is by using probabilistic methods. Bulthuis et al. (2019) introduced two characteristic relaxation times for East and West Antarctica. An uncertainty range was defined for both regions and the ice model was tested using this range of relaxation times. When including a range of relaxation times from a few decades to a few millennia, the contribution of the bedrock response to the change in global mean sea level is 10% (Bulthuis et al., 2019). This asks for a more sophisticated method to include lateral variation so that a wide variety of viscosities can be used on much smaller spatial scales.

Laterally varying visco-elastic Earth models, called 3D GIA models, compute deformation of the Earth's surface on a spatial resolution of several to a few hundred kilometers. Deformation can be determined analytically for a homogenous stratified Earth or a heterogenous stratified Earth with relatively low perturbations in viscosity (Tromp and Mitrovica, 1999). A numerical model such as the finite element method (FEM) or finite volume method is required to model a heterogenous Earth with relatively large perturbations in viscosity to solve for the Earth's response to loading.

Numerical 3D GIA models are computationally expensive. To reduce computational complexity and time, the ice load applied on the Earth model is prescribed and not dependent on the bedrock deformation. Thus, excluding the stabilizing GIA feedback effects. However, a recent study from Gomez et al. (2018) developed a method to include the feedback effect between GIA and ice load. A 3D, finite volume sea level and Earth deformation model were used to simulate the evolution of the Antarctic ice sheet using the following iterative method.

First, the sea level model simulates the period 40,000 years BP till modern date. Second, the GIA model ran the same period, using the ice load history provided by the sea level model. The topography used in the sea level model was adjusted based on the difference between the computed present day topography and the observed present day topography. Third, the sea level model simulates the full period using the new topography. The iterations are continued until the computed present day topography equals the observed topography. The results show significant differences in local ice thickness between the simulations using 3D GIA and 1D GIA (Gomez et al., 2018).

The coupling approach from Gomez et al. (2018) couples the ice dynamic and sea level model at a timescale of 40,000 years. However, the feedback effect occurs continuously, forced by large changes in deformation and ice thickness at timescales of 500 to 5000 years (Konrad, 2015). It would therefore be interesting to include the feedback effects in a coupled model at timesteps smaller than 40,000 years. Since no current method exists that allows for iterations at relatively small timesteps, this asks for the development of a new method that includes the GIA feedback effects.



In this study, a new method has been developed using a forward modelling approach to allow for simulation of the ice evolution including the GIA feedback effect by iterating an ice dynamic and GIA model at relatively small timesteps. The used ice-sheet-shelf model is ANICE. The research group Institute for Marine and Atmospheric research in Utrecht, The Netherlands, developed an ice-sheet-shelf model called ANICE (de Boer, 2013). Relatively small adjustments had to be made to include bedrock deformation from the GIA model instead of computing bedrock deformation using the ELRA model. More information about ANICE and the modifications that are done can be found in Appendix A.

The used GIA model is a numerical 3D GIA model based on the FEM using a prescribed ice load, developed by the research group at the Faculty of Aerospace Engineering at the Technical University of Delft, The Netherlands (Hu et al., 2017; Blank, In prep). Adjustments had to be made to make the model suitable for forward modelling, to restart timesteps and to use a dynamic ice load input instead of a prescribed ice load input. This is done using the restart concept developed by Weerdesteijn (2019). More information about the GIA model and the modifications that are done can be found in Appendix B.

Developing the new method and applying the method allows to study GIA feedback effects in such detail that could not be done using any other model but introduces problems that asks for extensive testing and analysis to find a suitable solution. For instance, the resolution and the type of grid of ANICE and the FEM model differ. An interpolation method is needed to interpolate ice and ocean load from the ANICE grid to the FEM grid and to interpolate the deformation from the FEM grid to the ANICE grid. Also, an iterative process is needed to include GIA feedback effects. Therefore, a convergence criterium must be defined to decide how many iterations should be performed. More information about the performed interpolation tests can be found in Appendix C and more information about the performed convergence tests can be found in Appendix D.

## 1.4 Research objective and questions

By developing the coupled model, research can be performed on the effect of GIA feedbacks on ice dynamic characteristics over the past 120 000 years for the AIS. By knowing the effect of GIA feedback on local ice dynamics, better uncertainty estimates can be made for ice models that do not include the GIA feedback effects and for ice models that use prescribed ice loading.

The goal of this study is to present a new method to fully couple an ice- and 3D GIA model at timescales of 1000 to 5000 years for the AIS. The model assesses the impact of a forward modelling coupling approach using a 3D rheology on the ice sheet evolution, compared to a laterally homogeneous rheology. The developed coupled model can be used to provide present day uplift rates on a high resolution to improve the correction for ongoing GIA to modern geodetic data.

The analysis of the results will be useful for future modelling of the AIS evolution and for improving the accuracy of GIA models for Antarctica. The coupled model could contribute to a more precise simulation of the evolution of the AIS and to better estimates of the present-day ice sheet characteristics and GIA effect. Better estimates for GIA and ice sheet characteristics will ultimately lead to better calibration of forecasting models and a more precise correction for ongoing GIA to modern geodetic data.

The main research question is:

- What is the effect of the interaction between Glacial Isostatic Adjustment and ice sheet dynamics on the Antarctic Ice Sheet growth during the last glacial cycle?

To be able to answer the main question, several underlying questions need to be answered:

- How can the GIA FEM model and ANICE be coupled?



- What is the accuracy of the method?
- What are the differences in ice sheet thickness, grounding line position and deformation when using a laterally varying Earth structure compared to a laterally homogeneous Earth structure for the Antarctic Ice sheet?

Section 1 provides background information about the geology of Antarctica, the history of the AIS, the current state of the AIS, the ice dynamics occurring at Antarctica, the structure and deformation of the solid Earth at Antarctica and the current models that are used to simulate the evolution of the AIS.

Section 2 includes the first draft of the article that is written from this study. The article includes an introduction (unavoidably, some overlap with section 1 occurs), a description of the method that is developed and applied on an ice model and GIA model, a presentation of the most important results to compare ice volume and ice growth using a coupled model with 1D viscosity of the Earth and 2 types of 3D viscosity. Due to time constraints, present day results of the coupled model will be shown using a 1D rheology. The first timestep, 120,000 to 115,000 BP, is analyzed in detail using two different 3D rheologies. The article concludes with the discussion of the results and recommendations for future studies. The reference section at the end of the article includes all references of the report. Since the developed method is complex and a completely new approach, supplemental figures are provided to further clarify the developed method.

Section 3 is a general conclusion explicitly answering the research questions. Appendices are added to this report to provide more information about the models and the method. More information about the setup of the ice dynamic model, ANICE, that is used to compute the ice sheet evolution is provided in Appendix A. More information about the development and set up of the finite element model used to compute the deformation of the Earth's surface is provided in Appendix B. The coupling of the ice and the GIA model asks for interpolation of the results of each model. Appendix C is describing the interpolation method used in this study. Appendix D is providing more details about the developed method. The developed method is tested and verified extensively. A presentation of the test results can be found in Appendix E.



2

Article

# A new method to simulate the Antarctic Ice sheet over the last glacial cycle using a 3D GIA - Ice Dynamic model coupled at thousand-year timescale intervals

Caroline van Calcar<sup>1</sup> et al.

5 <sup>1</sup>Faculty of Civil Engineering and Geosciences, Delft University of Technology, Delft, The Netherlands

*Correspondence:* Caroline van Calcar (carolinevancalcar@live.nl)

**Abstract.** A recent comparison of 15 ice sheet models projected that the Antarctic Ice Sheet (AIS) could contribute -7.8 to 30 centimeters of sea level rise between 2015 and 2100, meaning that sea level rise could increase a lot although the uncertainty is high (Seroussi et al., 2020). To better predict the future of the AIS, more accurate simulations of the evolution of the AIS  
10 are needed. Over glacial-interglacial cycles, the evolution of an ice sheet is influenced by Glacial Isostatic Adjustment (GIA) via two negative feedback loops. First, vertical bedrock deformation due to a changing ice load alters ice-sheet surface elevation. Second, bedrock deformation will change the location of the grounding line of the ice sheet. GIA is mainly determined by the viscosity of the interior of the solid Earth which is radially and laterally varying. Underneath the Antarctic Ice Sheet (AIS), there are relatively low viscosities in West Antarctica and higher viscosities in East Antarctica, which affect  
15 the response time of the above-mentioned feedbacks. However, most ice-dynamic models do not consider a laterally varying Earth structure when simulating the evolution of the AIS.

This study presents a new method to investigate 3D GIA feedback effects in detail at any chosen period during the last glacial cycle. The method is applied using ANICE and a 3D GIA FEM model. This led to the development of a fully coupled ice dynamic-3D GIA model with coupling timesteps of 1000 and 5000 years. Following the new method, the model  
20 computations alternate between the ice-sheet model, ANICE, and a 3D Finite Element Method model until convergence of the ice thickness occurs at each timestep. We simulate the evolution of the AIS from 120 000 years before present to modern date, considering 1D and non-linear 3D rheologies.

The maximum difference between the uncoupled deformation (iteration 1) and the coupled deformation (average between the last two iterations) for the period 120,000 to 115,000 years BP is 3 to 8 mm per year, depending on the viscosity  
25 of the upper mantle. The increases in deformation using a 3D wet rheology with a grain size of 10 mm are highest at the Siple Coast, the Ronne Ice Shelf, and several other locations along the grounding line of the AIS. The maximum difference in ice thickness at 115,000 years BP is 50 meters close the Ronne Ice Shelf and the Ross Ice Shelf. The grounding line position differs up to 80 meters when applying the coupling method compared to the uncoupled result. The results of this study emphasize the importance of the 3D GIA feedback effects when simulating the evolution of the AIS during the last glacial.

## 30 1 Introduction

Sea level rise has a high impact on society and the improvement of forecasts are vital to generate both adaptation and mitigation strategies and help policymakers decide on what investments should be done to protect people and the environment (Oppenheimer, 2020). A recent comparison of 15 ice sheet models projected that the Antarctic Ice Sheet (AIS) could contribute  
35 -7.8 to 30 centimeters of sea level rise between 2015 and 2100, meaning that sea level rise could increase a lot although the uncertainty is high (Seroussi et al., 2020). To better predict the future of the AIS, more accurate simulations of the evolution of the AIS are needed.

Due to the declining bedrock elevation towards the center of Antarctica and the large ice volume of the AIS, the Antarctic collapse could increase future sea level rise severely (DeConto & Pollard, 2016). Glacial isostatic adjustment (GIA) changes

the bedrock topography and thus influences the evolution of the ice sheet. Several models are developed to include GIA in ice dynamic models. Firstly, changes in bedrock topography due to load can be included in an ice dynamic model using the Elastic Lithosphere Relaxing Asthenosphere model (ELRA) (Le Meur & Huybrechts, 1996). This is a two-layer model that contains a local elastic lithosphere and a relaxing asthenosphere using a constant relaxation time. This simplified model is effective in computing the bedrock response and therefore favorable to compute the evolution of an ice sheet on long timescales.

Secondly, self-gravitating visco-elastic spherical Earth models compute the complete Earth composition with radially varying Earth models (1D GIA models), accounting for gravity field perturbations and displacements using spherical harmonics. When a load is placed on a visco-elastic body, the body deforms to stress as a function of viscosity, density, and elastic parameters. Rheological models are used to describe the relation between stress and strain. There are two ways to calculate the spatially time-dependent response of the Earth to surface load. First, The Maxwell rheology assumes the Earth is a linear viscoelastic body. The response can be calculated using viscoelastic Love numbers. These Love numbers reflect the assumed viscosity profile of the mantle. Second, the power-law approach (Wu, 1998) assumes the Earth is a nonlinear viscoelastic body where the effective viscosity depends on the stress field throughout the mantle, which depends on the surface load change. Non-linear stress-strain relationships form the basis of the power-law approach. Grain scale deformation of mantle material is described by diffusion and dislocation creep. These parameters describe a nonlinear relationship where strain rate depends on stress. This relation is dependent on grain size, water content, melt content and temperature.

The relaxation time is shorter for lower viscosity's in the mantle. GIA models with radially and laterally varying viscosity (3D GIA models) show several orders of magnitude difference in relaxation time (Gomez et al., 2018). Since the viscosity of the mantle of the Earth laterally varies with three orders of magnitude in Antarctica, the uplift is underestimated in west Antarctica and overestimated in east Antarctica (Heeszel et al., 2016). Deformation can be determined analytically for a homogenous stratified Earth or a heterogenous stratified Earth with relatively low perturbations in viscosity. A numerical model such as the finite element method (FEM) or finite volume method is required to model a heterogenous Earth with relatively large perturbations in viscosity to solve for the Earth's response to loading. Several models have been developed to simulate GIA using a lateral variable rheology in Antarctica (Kaufmann et al., 2005; A et al., 2013, van der Wal et al., 2015; Gomez et al., 2018). Blank et al (In prep) developed a 3D GIA model using the finite element method and the formulation from Van der Wal et al. (2013) to model the viscosity of the olivine (Hirth and Kohlstedt, 2003). The results of Blank et al. (In prep) show major differences in the use of 1D and 3D GIA models for the Amundsen Sea Embayment. Also, Hay et al. (2017) showed that the simulated Antarctic collapse could be occurring faster than previously computed when including 3D GIA in the model. Grounding line migration plays an important role in sea level projections (Gomez et al., 2010).

The aforementioned ice-sheet models include 1D or 3D GIA effects but do not take into account the feedback effects following from the interaction between GIA and the evolution of the ice sheet. Namely, vertical deformation of the Earth's surface and a changing ice sheet thickness influence each other in two ways (Whitehouse et al., 2019). First, vertical deformation of the Earth's surface changes the surface elevation of the ice sheet directly. The surface of the ice sheet will be exposed to a change in snowfall and atmospheric temperature, leading to a change in growth or decay of the ice sheet.

Second, deformation of the Earth's surface will change the position of the grounding line of the ice sheet. A thinner ice sheet thickness as a result of surface melt leads to an increased ice flux towards the ice shelf. The thickness is proportional to the water depth, resulting in a large reduction in grounded ice caused by a small increase in water depth at the grounding line (Whitehouse et al., 2019). On its turn, a reduction in grounded ice leads to upward deformation of the Earth's surface and the local sea level lowers due to the diminishing gravitational attraction of the ice on the surrounding water (de Boer et al., 2017). The local shallowing of water reduces the loss of ice across the grounding line.

The effect of the GIA feedback on the grounding line migration is dependent on the deformation rate, the bedrock slope, and ongoing viscous uplift of the Earth's surface (Whitehouse et al., 2019). A lower sea level, because of the GIA feedback, reduces the ice loss around the grounding line. Therefore, the GIA feedback effect stabilizes, and in some cases halting,

migration of the grounding line along reversed bed slopes (Larour et al., 2019; Gomez et al., 2012). Ongoing viscous uplift of the bedrock could even initiate a readvance of the grounding line (Pollard et al., 2017).

Since bedrock deformation rates are highly dependent on the viscosity of the interior of the Earth, also the GIA feedback effect is dependent on the viscosity. The stabilizing GIA feedback effect is quick at regions containing relatively low mantle viscosities because the mantle approaches isostatic equilibrium 1-2 orders of magnitude faster compared with global-average timescales, resulting in high deformation rates (Whitehouse et al., 2019). The GIA feedback effects play an important role in regional ice sheet evolution of the AIS because of the strong relation with the viscosity of the Earth (Larour et al., 2019; Whitehouse et al., 2019; Pollard et al., 2017;).

The GIA feedback effects can be modelled using a coupled ice dynamic - sea level model by incorporating the sea level equation and visco-elastic love numbers (Larour et al., 2019; Konrad et al., 2015; de Boer, 2014; Gomez et al., 2013). The sea level model computes the bedrock deformation and the relative sea level change and forwards this to the ice sheet model. However, sea level models do not account for laterally varying mantle viscosities. The first model that couples 3D GIA with ice dynamics was developed by Gomez et al. (2018). Here, the method of Kendall et al (2005) was used to compute the self-consistent sea level for ice mass change. The estimation of the ice thickness of the present-day ice sheet is dependent on the evolution of the ice sheet over the past ten thousands of years, which on its turn depends on the viscosity of the interior of the Earth. Thus, an iterative method is necessary between the ice history and the Earth model. The current topography can be validated by the measured topography and this leads via multiple iterations to an improved estimated initial topography and thus an improved ice sheet evolution. The two models are separately running with a fixed ice load and bedrock elevation history as input. The total contribution from Antarctica to sea level change has not changed much over the last deglaciation by using a coupled 3D Earth rheology instead of a 1D rheology. However, local ice thickness differs up to 200 meters when using a 3D GIA model instead of a 1D GIA model, leading to differences in relative sea level up to 80 meters (Gomez et al., 2018).

The first coupling approach from Gomez et al. (2018) couples the ice dynamic and sea level model at a timescale of 40,000 years. However, the GIA feedback effects occur continuously, forced by large changes in deformation and ice thickness at timescales of 500 to 5000 years (Konrad, 2015). It would therefore be interesting to include the GIA feedback effects in a coupled model at timesteps smaller than 40,000 years. Since no current method exists that allows for iterations at relatively small timesteps, this asks for the development of a new method that includes the GIA feedback effects.

The goal of this study is to present a new method to fully couple an ice- and 3D GIA model at timescales of 1000 to 5000 years. The new method uses a forward modelling approach to allow for simulation of the ice evolution including the GIA feedback effect by iterating an ice dynamic and GIA model at relatively small timesteps. To approach the realistic process of continuous feedback, the deformation and ice thickness are calculated every 5000 years for the glacial cycle from 120,000 years before present (BP) to 20,000 years BP and every 1000 years for the period from 20,000 years BP to modern date.

The model is applied to the Antarctic region to assess the impact of a forward modelling coupling approach using a 3D rheology compared to a laterally uniform rheology. Last Glacial Maximum (LGM) and present day results of the coupled model will be shown using a 1D rheology. The first timestep, 120,000 to 115,000 BP, is analyzed in detail using two different 3D rheologies. The model can provide present day uplift rates on a high resolution to improve the correction for ongoing GIA to modern geodetic data. The iterative scheme of the developed method is presented in this study. The analysis of the results will be useful for future modelling of the AIS evolution and for improving the accuracy of GIA models for Antarctica.

## 2. Method

In this study we present the results of simulations in which we couple an ice-sheet-shelf model to a GIA model that incorporates 3D variation in the Earth structure. The simulation asks for global mean sea temperature and sea level timeseries, global mean atmospheric temperature timeseries, initial bedrock height, precipitation patterns, a geothermal heat flux map and 3D viscosity

maps of the Earth's interior. The two models and the coupling procedure are described below. The results of the first timestep for all three experiments is discussed in this article.

## 125 2.1 Ice dynamic model

The ice dynamic model adopted, "ANICE", is described in detail in de Boer et al. (2013) and in Appendix A of this thesis. ANICE is an ice-sheet-shelf model and is used in this study to simulate the Antarctic region at a resolution of 40 by 40 kilometers. Multiple experiments have been done using ANICE (Berends et al., 2019; Berends et al., 2018; Bradley et al., 2018, Maris et al., 2014).

130 The ice sheet evolution is dependent on several climate factors. Time- and latitude- dependent insolation at the top of the atmosphere varies on time scales of 120,000 years (Laskar et al., 2004). The global mean temperature and sea level are used as input to force the ice-sheet-shelf model. The global mean atmospheric temperature is decreasing with 14 degrees Celsius between 120,000 years BP and 20,000 years BP. From 20,000 years BP till present day, the temperature increases with 15 degrees Celsius to approximately 0. The assumed global mean temperature and sea level are shown in Figure S.1 in the  
135 supplementary materials.

The mass balance of the ice sheet is calculated using present-day monthly precipitation as a function of free atmospheric temperature (Bintanja et al., 2005; Bintanja & van de Wal, 2008). The mass continuity of the ice sheet is calculated with Equation (1) where  $H_i$  is the height of the ice,  $u$  is the vertically integrated horizontal velocity profile, computed by using Equation (2), and  $B$  is the mass balance per unit of time, computed by using Equation (3).

$$\frac{\partial H}{\partial t} = -\nabla \cdot (H_i u) + B \quad (1)$$

$$u = u_{\text{sliding}} + u_{\text{deformation}} \quad (2)$$

$$B = \text{precipitation} - \text{melt} \quad (3)$$

140 ANICE uses the shallow shelf approximation (SSA) (Bueler and Brown, 2009) to solve mechanical equations for ice shelf dynamics and the shallow ice approximation (SIA) to solve for grounded ice (Morland, 1987; Morland & Johnson, 1980).  $U_{\text{deformation}}$  is determined using the SIA, whereas sliding and ice-shelf velocities are calculated using the SSA.

A surface temperature-albedo-insolation parameterization is used to calculate ablation (Laskar et al., 2004). Global mean sea level and a combination of the temperature-based formulation by Martin et al. (2011) and the glacial-interglacial  
145 parametrization by Pollard and DeConto (2009) is used to compute sub-shelf melt. The results are tuned to produce realistic present-day Antarctic shelves and grounding lines (de Boer et al., 2013). Sub-shelf melt and grounding line migration effect calving. Calving is included in the model by removing ice shelf with a thickness lower than 200 meters.

The initial topography at 120,000 years BP is taken from BEDMAP2 (Fretwell et al., 2013). GIA directly influences the surface height of the ice sheet and thus the precipitation and the mass balance. GIA affects sub shelf melt and grounding line  
150 migration as well due to a changing sea level. ANICE is adjusted for this study to include input of the GIA finite element model. The average deformation for one timestep of 5000 or 1000 years is computed by the coupled GIA model and linearly applied to the ice model at timesteps of 100 years.

## 2.2 GIA model

The adopted GIA model for this study is a numerical 3D GIA model based on the finite element method using a prescribed ice  
155 load (Hu et al., 2017; Blank, In prep). The finite element method (FEM) is the numerical method used in this study to determine displacements in the Earth model under surface loading and is chosen for its computational effectivity. The concept of a GIA model based on a commercial FEM was developed by Wu (2004) and applied using the software ABAQUS (Hibbitt et al.,

2016). FEM is applied in several experiments, for example using a flat Earth model to simulate the West Antarctic Ice Sheet (Nield et al., 2018) and a spherical Earth model for Fennoscandia (van der Wal, 2013).

160 It is assumed that the Earth is in isostatic equilibrium at the start of the simulation at 120,000 years BP, neglecting the ongoing deformation in response to the previous glacial cycle to reduce simulation time. The modelled sphere consists of 6 layers, one layer representing an inviscid core, four layers representing a viscoelastic lower and upper mantle and one layer representing an elastic crust, and is divided in an irregular grid with an approximate resolution of 200 by 200 kilometers at the surface. This can be scaled up to a higher resolution, but this increases the computation time.

165 The input for the GIA model is the ice and ocean load. The ice load is linearly interpolated from a regular grid of 0.25 degrees latitude by 0.25 degrees longitude to the irregular grid of the modelled sphere. The applied load causes stresses in the Earth model. The FEM allows for modelling of deformation and stresses in the Earth using a modified stiffness equation and Laplace's equation (Wu, 2004). These equations for a self-gravitating incompressible spherical Earth model are transformed to boundary conditions for each layer using the method from Wu (2004).

170 Self-gravitation of the ice sheet and its effect on sea level, as well as the load from the North American, Eurasian and Greenland ice sheets is included in the coupled model but is not coupled to the GIA, nor is the ice dynamic model. Global relative sea level is computed using the ice history from Whitehouse et al. (2012) and a 3D rheology based on the seismic model from Schaeffer and Lebedev (2013) globally, and Heeszel et al. (2016) over Antarctica. The relative sea level is linearly decreasing between 120,000 years and 20,000 years BP, corresponding to an assumed linear increase of ice mass. The  
175 computed relative sea level is interpolated to the timesteps used in this study and applied as a load on the GIA model.

The impact of lateral variations in lithospheric thickness and viscosity on GIA in West Antarctica is high (Nield et al., 2018). Lateral and radial variations of the Earth's mantle can be described by a combination of linear and non-linear viscoelastic behaviour, called the composite rheology. Diffusion creep, corresponding to linear viscoelasticity, and dislocation creep, corresponding to the non-linear relation between shear stress and strain rate, are components of the composite rheology  
180 and can be defined by the diffusion and dislocation creep parameters, respectively (Hirth and Kohlstedt, 2003).

The dislocation and diffusion parameters used in this study are determined using the flow law from Hirth and Kohlstedt (2003) (van der Wal et al., 2013). Dislocation and diffusion parameters are derived from seismic models. Velocities anomalies are used to create an average of three seismic models (Becker & Boschi, 2002). Seismic velocity anomalies are converted to temperature, assuming that all seismic velocity anomalies are caused by temperature variations (Goes et al., 2000). Derivatives  
185 of seismic velocity anomalies to temperature anomalies are provided as a function of depth in Karato et al. (2008). The temperatures are converted to absolute temperatures and used in a flow law to obtain creep parameters (van der Wal, 2013). All parameters except grain size and water content are taken from Hirth and Kohlstedt (2003).

The FEM model allows for assigning dislocation and diffusion parameters to each grid cell, which makes the model suitable to compare different 1D and 3D rheologies. The effective viscosity is computed for each grid cell using Equation (4)  
190 where  $B_{diff}$  and  $B_{disl}$  are the diffusion and dislocation parameters respectively,  $q$  is the von Mises stress, being  $q = \sqrt{\frac{3}{2}\sigma'_{ij}\sigma'_{ij}}$  and assumed to be 0.1 Mpa, and  $n$  is 3.5 being consistent with Hirth and Kohlstedt (2003) (van der Wal et al., 2013).

$$\eta_{eff} = \frac{1}{3D_{diff} + 3B_{disl}q^{n-1}} \quad (1)$$

Compressibility effects and the influence of sediment loading are not included in the GIA model as the interest of this study is the first-order effect of viscosity variation. Centrifugal effects flatten the Earth's shape at the poles. However, the  
195 curvature of the Earth's surface is small when focusing on the area of Antarctica, so this flattening effect has negligible effects on GIA and is therefore not included in the model.



Adjustments had to be made to make the model suitable for forward modelling, to restart every timestep several times and to use a dynamic ice load input per timestep instead of a prescribed ice load input at all timesteps. Therefore, the new model is rebuild using a restart concept developed by Weerdesteijn (2019). There, the model runs several iterations per timestep using a restart job. However, the model developed by Weerdesteijn (2019) is solely used to study the effect of polar wander on GIA, using a constant prescribed load without the possibility to stop after each timestep. Therefore, also this concept needed adjustments to allow for computation of only one timestep and to save all output needed for the next timestep. The output of the model provides, among others, radial displacement per timestep at the surface and the model database of the deformed Earth to use for the next timestep. More information about the GIA model and the modifications that are done can be found in Appendix B of this article.

## 2.3 Coupling method

ANICE and the GIA model are coupled using the forward modelling method to study the feedback effects between the evolution of the AIS and 1D and 3D GIA effects. The simulation starts at 120,000 years BP and iterates between the ice and GIA model until present day in fixed timesteps of 5000 years (120,000 years BP till 20,000 years BP) and 1000 years (20,000 years BP till modern date).

The simulation of ice dynamics for a certain timestep requires the deformation over the timestep. On the other hand, the computation of the deformation at this timestep, using the GIA model, requires the change in ice mass at that timestep. This asks for an iterative process. For the first timestep, the deformation is taken from an uncoupled ANICE simulation using ELRA. The final deformation of the timestep is taken as the initial guess for the next timestep. The iterative process where alternating simulations of the ice dynamic model and the GIA are done at every timestep is continued until convergence in deformation has been reached.

The models compute the output on a different grid. Therefore, interpolation of the output is needed to use the output of one model as input for the other model. Oblimap is used to apply the quadrant method and the radius method to the data because the program works computationally fast and provides a very detailed result (Reerink et al., 2016). The quadrant method is used for gridding from a coarse grid to a fine grid. The region around the grid point of the fine grid is divided in four quadrants. The Shepard distance-weighted averaging is applied to the most close by coarse grid points in each quadrant using a Shepard's power parameter of 2. A lower parameter will result in a smoother output but also less detailed.

The radius method is used for gridding from a fine grid to a coarse grid. In case of a relatively coarse grid size, all fine grid points within a radius of the order of half the coarse grid size are included by a Shepard distance-weighted averaging interpolation method to obtain a representative value for this grid point. Detailed information about Oblimap and about the motivation for the choice of this interpolation can be found in Appendix C of this article.

### 2.3.1 Iterative coupling process

The iterative scheme is shown in Figure 1. The ice thickness and deformation at each timestep of the coupled model is computed as follows:

1. The initial topography and deformation are used as input for ANICE. The ice evolution is computed for the first timestep.
2. To compute the load used by the GIA model, the initial grounded ice thickness is subtracted from the grounded ice thickness at the end of the timestep and multiplied by the density of ice (assumed to be  $931 \text{ kg/m}^3$ ). The ice load is added to the relative sea level change from the W12 model and multiplied by the density of water (assumed to be  $1000 \text{ kg/m}^3$ ).

3. The total load is passed to the GIA model. The model computes the deformation of the Earth's surface for that timestep. The deformation is passed to ANICE and divided by the length of the timestep to obtain annual deformation. ANICE computes the new ice evolution for the timestep using the annual deformation.
- 240 4. The iterative process described in step 3 continues until the convergence criterium, that is the difference in deformation between iterations is smaller than 2 mm/year, has been met. The convergence criterium is described in section 2.3.2. The average deformation of the last two iterations is taken as the final deformation to minimize the uncertainties in areas where the model does not converge to zero but alternates between positive and negative values. The average deformation is passed to ANICE to calculate the final ice sheet evolution over the current timestep.
- 245 5. The average deformation will be used as initial guess and the final ice thickness and bedrock height will be used as initial values for the next timestep (used in step 1). The Finite Element Model includes the stresses introduced by former timesteps in the model at the new timestep.

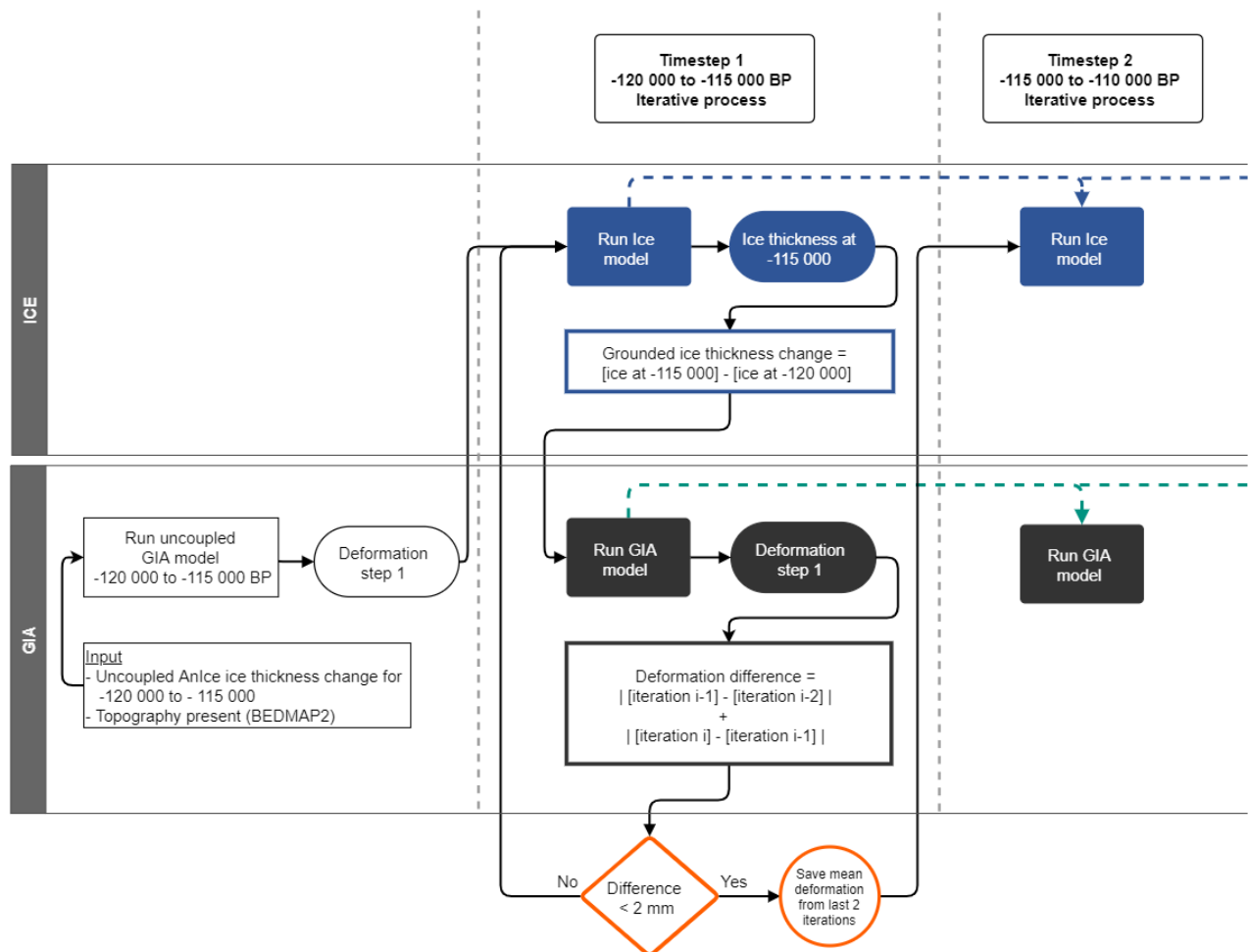


**Figure 1: Schematic overview of the developed forward coupling method. It is shown that several iterations occur within one timestep until the convergence criterium of a maximum difference of 10 meter of deformation has been met for all elements of the GIA model.**

### 2.3.2 Convergence of the timestep

The coupled model requires three to four iterations per timestep to converge when using a 1D rheology with a viscosity of  $1 \cdot 10^{21}$  Pa·s for the upper mantle. The exact amount of iterations needed to convergence is dependent on the change in ice load. A high deformation rate and large changes in ice thickness affect the position of the grounding line. Glaciated grid cells of the ice dynamic model are defined as grounded ice or floating ice dependent on the grounding line. If the grounding line in the ice model keeps moving at every iteration due to high changes in deformation, the ice load transferred to the GIA model keeps alternating between no load and thick ice load at grid cells around the moving grounding line. In this case, deformation in these grid cells does not converge to zero. However, an alternation of the same negative and positive value is reached for these

locations. Such an alternation occurs for example in the Antarctic Peninsula at the timestep 95,000 till 90,000 years BP when using a 1D rheology. The difference in deformation and load between iterations of this timestep is shown in Figure S.2 of the supplemental material.

260 Since ice thickness can differ a lot between adjacent grid cells, the changes between iterations can also be big. Deformation converges better than ice thickness because of the smoothness of the deformation signal. To determine if the timestep is converged, the difference between the last iteration and the last one iteration is added to the difference between the last one and the second last iteration. The chosen convergence criterium detects when all grid cells have converged to a maximum of 2 mm per year where certain grid cells have been alternating between the same positive and negative value. The average deformation of the last two iterations is used to compute the final ice load. Two convergence criteria are tested and described in section D.1 of Appendix D.

270 A small timestep is desirable to increase the number of grid cells converging to zero. On the other hand, a large timestep is desirable to decrease the computation time. Tests were done with 3 different timesteps of 1000, 2500 and 5000 years using the 1D rheology. A timestep of 5000 years is chosen for two reasons. First, the GIA signal is not expected to change a lot within this period, although the deformation is highly dependent on the chosen mantle viscosity. Second, a timestep of 5000 years is big enough to converge within 3 iterations to prevent an extremely long computation time. Since the change in ice load in the deglaciation period is much bigger, a smaller timestep of 1000 years was chosen for this period.

## 2.4 Experiments

Three experiments are done to analyze the performance of the coupled model:

- 275 1. Computation of the ice sheet evolution using a 1D GIA model. The viscosity of the upper mantle and the asthenosphere is set to  $1 \cdot 10^{21}$  Pa · s.
2. Computation of the ice sheet evolution using a 3D dry rheology model.
3. Computation of the ice sheet evolution using a 3D wet rheology model.

280 The chosen 1D viscosity is shown in Figure 2A. The chosen 3D rheological models shown in Figures 2B and 2C represent realistic viscosity values derived from seismic models (van der Wal et al., 2013). It can be seen that the commonly used 1D rheology is up to 2 orders of magnitude higher than viscosities derived from seismic data in West Antarctica and 1 to 2 orders of magnitude lower than viscosities derived from seismic data in East Antarctica. The viscosities for the dry rheology with 4 mm grain size (Figure 2B) is approximately one order higher than the viscosities for the wet rheology with 10 mm grain size (Figure 2C).

285 The initial load and climate conditions are equal for the three tests. During the period 120,000 to 115,000 years BP, it is assumed that the mean global atmospheric temperature decreases with approximately 1.5 degrees Celsius per 1000 years. The sea level decreases relatively less with 1 mm per year, compared to 20 mm per year in the next period from 115,000 to 110,000 years BP. The global mean sea level and atmospheric temperatures are shown in Figure S.1 and the initial load is shown in Figure S.3 in the supplemental materials.

290

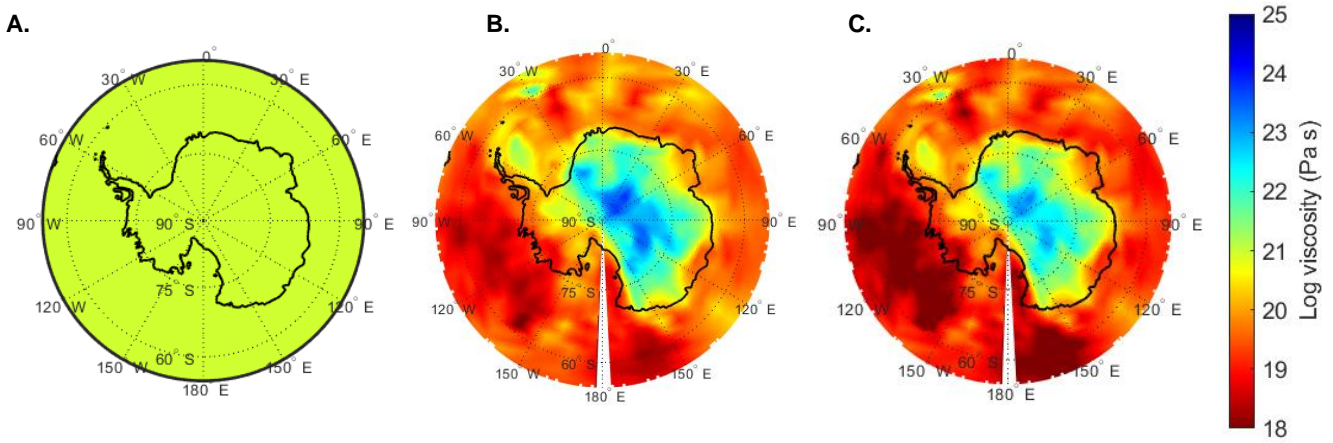


**Figure 2: Differences between 1D and 3D rheologies of which the viscosity is shown in Figures A-C at a depth of 246 kilometers. Figure A corresponds to the 1D rheology. The blue ellipse encircles the Siple Coast. Figure B corresponds to a dry rheology with a grain size of 4 mm. Figure C corresponds to a wet rheology with a grain size of 10 mm.**

295 **2.4.1 Main assumptions and uncertainties**

*Relative sea level*

The relative sea level is computed assuming a linear growth of the AIS between 110 000 years and 20 000 years BP. This is not consistent with non-linear growth of the AIS computed by ANICE during this period. As a result, the ocean load and the effect of self-gravitation are underestimated in the beginning of the period and overestimated at the end of the period. However, the effect of self-gravitation, the ocean load and the change in mass from other ice sheets globally on deformation at Antarctica is relatively small compared to the load of the AIS. Consequently, the uncertainties following from this assumption are small as well.

*Application of load and deformation on models*

For this study, it is assumed that the ice growth and deformation change linearly over time within one timestep. However, the deformation and ice dynamic equations are both solved on much smaller timescales and are nonlinear. When applying a load linearly over time, the deformation is lower until a constant rate is reached. In this study, the average deformation rate over the whole timestep is used as input for ANICE, where deformation is linearly applied every 100 years. Therefore, the deformation is slightly overestimated at the beginning of the timestep. This effect is higher at locations with a higher viscosity of the mantle due to a longer relaxation time and thus a longer time to reach a steady state (Barletta, 2018). Also, the ice dynamics computed by ANICE result in a nonlinear decay or growth dependent on the change in temperature and sea level forcing within the timestep. This is done using a dynamic timestep. In this study, the total change in grounded ice thickness is taken and applied on the FEM model linearly over time. This over- or underestimates the ice thickness, dependent on the temperature and sea level forcing at that time.

315

*Convergence*

Since the timesteps often not converge to approximately zero but to alternating values, this method introduces an uncertainty range that should be considered. For example, if in one grid cell the total deformation over 5000 years keeps alternating between -15 and 15 meters, the uncertainty range is 30 meters. The average of the last two iterations is taken to decrease the uncertainty range by 50 percent. The chosen allowable uncertainty range is 2 mm/year per timestep. The uncertainty introduced by the convergence criterium can be determined for every grid cell at every timestep. Adding these uncertainties per grid cell over time reveals which areas are highly uncertain.

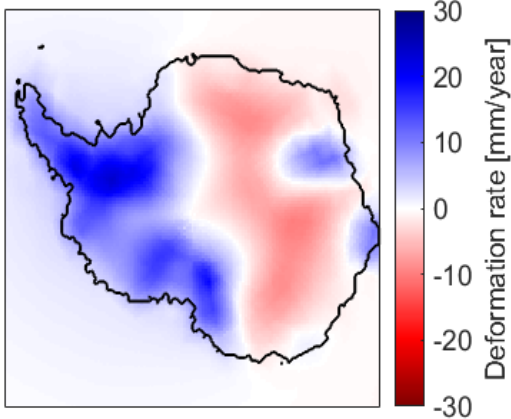
320

### 3. Results

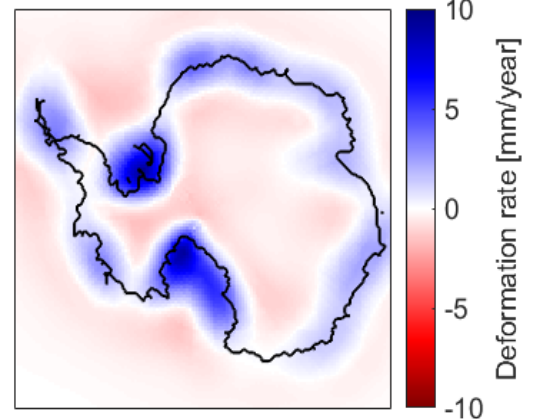
The coupled model has been used to simulate the full glacial cycles with a 1D Earth structure. The cooling trend in atmospheric  
325 temperature over the first 100,000 years of the simulation and the decrease of global mean sea level during this period (Figure  
S.1 in the supplemental materials) caused an extensive growth of the AIS. The atmospheric temperature and the global mean  
sea level rose between 20,000 years BP and present day, causing an ongoing melting epoch of the AIS. This results in a  
retreating grounding line, which can be observed when comparing the black line in Figures 3A and 3B.

The average vertical deformation around the LGM varies with 40 mm per year across Antarctica (Figure 3A). The average  
330 vertical deformation over the past 1000 years varies with 20 mm per year across Antarctica (Figure 3B). The deformation  
changed from negative to positive around the grounding line in large parts of East Antarctica. The present day bedrock height  
resulting from the coupled model simulation using a 1D rheology is similar to the present day observed bedrock height from  
BEDMAP2 with a maximum difference of 10 meter at the Ross Ice Shelf and the Ronne Ice Shelf close to the present day  
grounding line (Fretwell et al., 2013).

A. 20 000 to 19 000 years BP



B. 1000 to 0 years BP



335

**Figure 3: Mean deformation rate over a certain timestep. Figure A shows the mean deformation rate over the period 20,000 years to 19,000 before present. Figure B shows the mean deformation rate over the last 1000 years until modern date. Note that the scales are different.**

#### 3.1 The effect of 3D viscosity

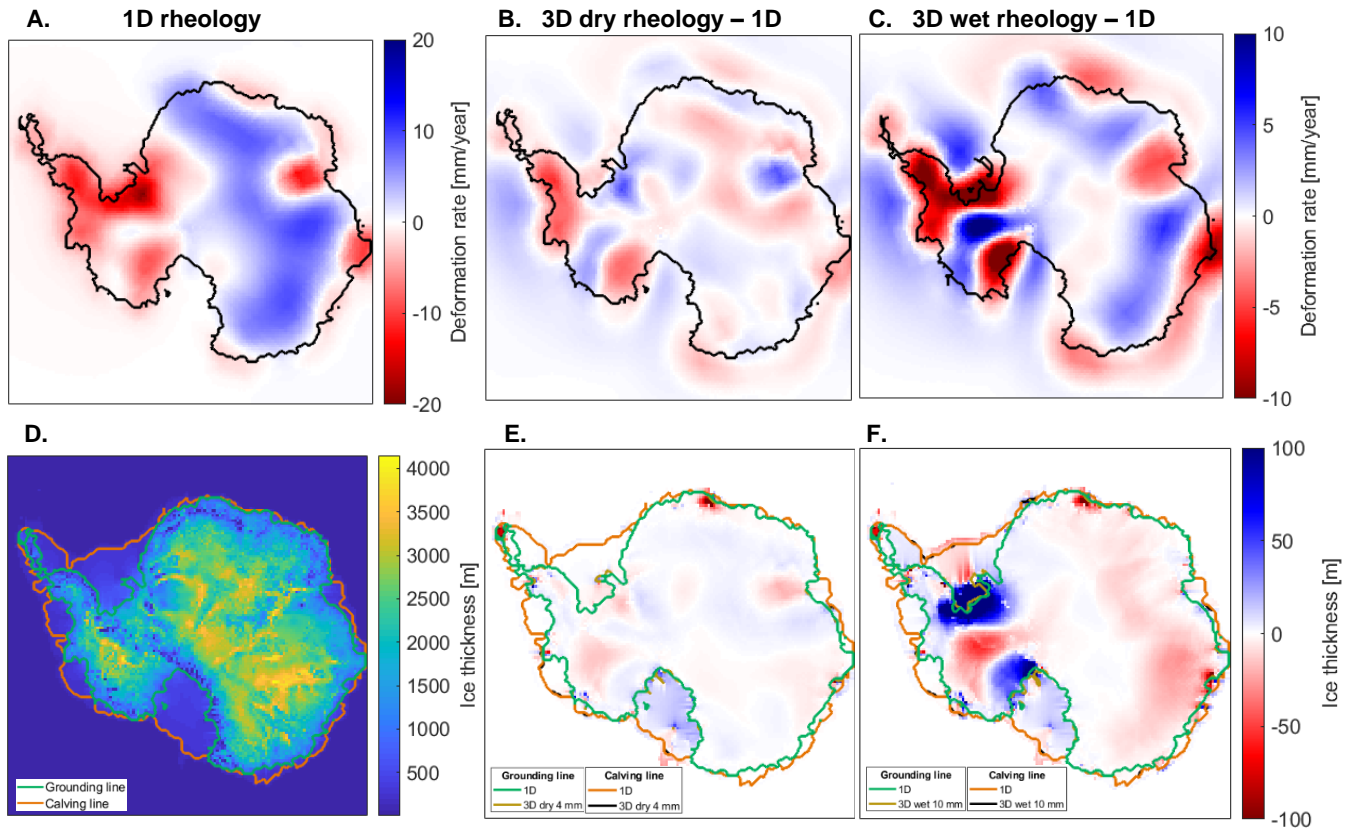
The results of the 3D coupled model are discussed in detail in this section for the period 120,000 years to 115,000 years BP  
340 using three different Earth structures introduced in the method section. To be able to study solely the effect of using a different  
rheology, the deformation is computed using an isostatic Earth model and the same ice load is applied at the start of the coupled  
simulations (Figure S.3 in the supplemental materials). The resulting deformation is used to simulate changes in ice thickness  
using the same climate forcing.

The assumed ice mass loss (Figure S.3 in the supplemental materials) is maximum at the Ronne Ice Shelf causing a local  
345 deformation of maximum 20 mm per year using a 1D rheology (Figure 4A). Considering the 3D dry rheology, the viscosity in  
West Antarctica is lower when using the 3D dry rheology than using the 1D rheology (Figure 2A and 2B) and therefore the  
negative deformation increases at the Ronne Ice shelf and even doubles at some locations in the peninsula (Figure 4B). On the  
other hand, the viscosity is higher in East Antarctica when comparing the 3D dry rheology with the 1D rheology. This leads  
to a lower deformation rate in East Antarctica for the 3D dry rheology compared to the 1D rheology (Figure 4B).

350 For the wet rheology, the viscosities beneath West Antarctica are even lower compared to the dry rheology. Therefore, the  
deformation increases compared to the 1D rheology (Figure 4). The deformation rate increases at the Antarctic Peninsula, the  
Ronne Ice Shelf and the west side of the Ross Ice Shelf from maximum 20 mm per year to maximum 30 mm per year when

using the 3D wet rheology instead of the 1D rheology (Figure 4C). There are locations in East Antarctica where the deformation doubles from approximately 10 mm per year to 20 mm per year (Figure 4C).

355 The differences in deformation when using different Earth structures lead to differences in ice thickness between 1D and 3D rheologies as well. At regions where the viscosity of the wet rheology is lower than the viscosity of the dry rheology, the difference in ice thickness between the two 3D rheologies is the highest (Figures 4D-F). The ice thickness is more than 100 meters higher at the Ronne Ice Shelf and the western side of the Ross Ice Shelf when using the wet rheology compared to using a 1D earth structure (Figure 4F). Also, the ice thickness differs by 50 meters in East Antarctica. Thus, lower viscosities  
360 of the Earth's mantle result in a bigger change of ice thickness and deformation over time.



365 **Figure 4:** Figures A-C show the deformation of the Earth's surface when applying the same load using the 3 different rheologies at the first timestep from 120,000 years to 115,000 years before present. Figure B and C show the difference with Figure A. The grounding line is shown with the black line. Figures D-F show the effect of the change in deformation on ice thickness where Figures E and F show the difference between the 3D simulation and the 1D simulation. The green and orange line correspond to the grounding and calving line, respectively. A yellow grounding line and a black calving line are shown in Figures E and F at locations and correspond to the line resulting from the 3D rheology. Note that the black and yellow line are only visible around the Ronne Ice Shelf and the Ross Ice Shelf.

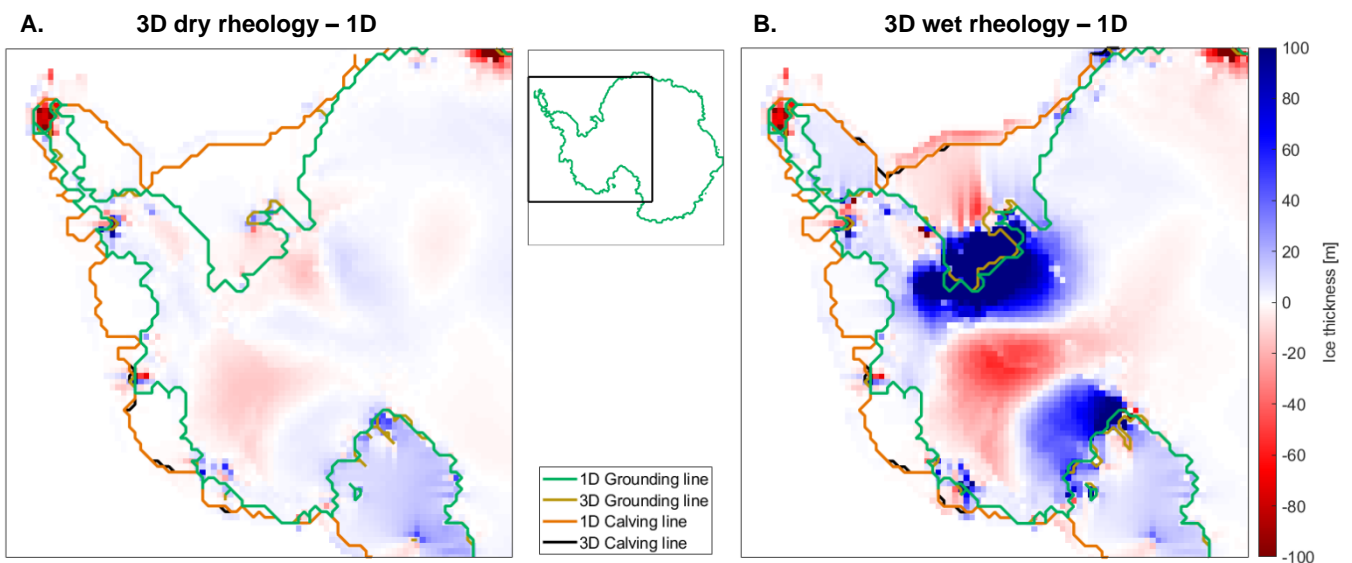
The green and orange lines in Figure 4D show the grounding line and the calving line respectively at 115 000 years BP. These lines are shown in Figures 4E and 4F as well, together with the yellow grounding line and black calving line corresponding to the 3D simulation. Note that the black and yellow lines are only visible around the Ronne Ice Shelf and the Ross Ice Shelf. At several places at the Ross Ice Shelf and the Ronne Ice Shelf, the ice shelf can be 1500 meters thick very close to the grounding line. If the grounding line migrates toward the ice shelf with 40 kilometers per 5000 years, the ice load on the Earth's surface increases with approximately 1,500,000 kg per m<sup>2</sup> causing a subsidence up to 40 mm/years when using  
375 a wet 3D rheology with a grain size of 10 mm. There is a considerable ice mass transported towards the ice shelf when taking into consideration horizontal velocities of the ice mass of up to 1 kilometer per year, for example at the Lambert Ice Shelf.

At most locations, the calving and grounding line do not change more than 20 kilometers when using different 1D and 3D rheologies. However, local grounding line position variances of more than 20 kilometers do exist. The differences in ice thickness and grounding and calving lines in West Antarctica between the 1D rheology and the 3D rheologies are shown in



380 detail in Figure 5. The grounding line differs at places where the ice thickness decreases or increases with more than approximately 50 meters. The grounding line only changes over time at places where the change in ice thickness over time is big or at regions with high horizontal velocities of ice. For example, at the Lambert Ice Shelf in East Antarctica, where the topography is deep, and the ice flow is fast.

The calving line differs only at places where the ice thickness change over time passes the critical calving point of 200  
385 meter. Since the difference in ice thickness between using the 1D and the 3D dry rheology is almost nowhere higher than 50 meters, there is almost no difference in grounding line migration between the 1D and 3D dry rheology (Figure 5A). The grounding line difference between the 1D rheology and 3D wet rheology can go up to 200 kilometers at locations where the difference in ice thickness is 100 meters or more, such as the Ross Ice Shelf and the Ronne Ice Shelf (Figure 5B). At places where the ice thickness difference between 1D and 3D wet rheology is approximately 50 meters, the grounding line differs  
390 with approximately 50 kilometers (Figure 5B). An outward grounding line migration of 80 meters at the Siple coast due to ice thickening affects deformation due to the increase of grounded ice load of maximum 950,000 kg per m<sup>2</sup>. The results show an increase in ice load of a maximum of 1,500,000 kg per m<sup>2</sup> due to grounding line migration.



395 **Figure 5: Close up at grounding line migration differences between the 1D simulation and the 3D simulations. Figure A shows the difference in grounding line migration and ice thickness between the 1D simulation and the 3D dry simulation. Figure B shows the difference in grounding line migration and ice thickness between the 1D simulation and the 3D wet simulation.**

### 3.2 The effect of coupling an ice dynamic model to a GIA model on the Ross Sea embayment

The results of the simulation of the first timestep from 120,000 years to 115,000 years BP show that deformation of the Earth's  
400 surface does not influence whether the ice mass grows or decays, independent of the different rheologies that are tested (Figures 2A-C). However, the deformation does have an important impact on the rate of change of the ice mass balance, depending on the viscosity. This section describes the effect of each iteration on ice thickness and deformation for the Ross Sea embayment and shows results when using the 3D wet rheology for the coupled model

The Ross Ice Shelf is bounded by the Transantarctic Mountain range on the eastside and by the Siple Coast on the westside.  
405 The bedrock elevation under the Ross Ice Shelf is approximately 500 meters below sea level. The bedrock elevation of the Siple Coast is more complex (Fretwell, 2013). The bedrock has a retrograde slope that goes down to 2500 meters below sea level at the northern part of the Siple Coast and a prograde slope going up to 3000 meters above sea level at the southern part of the Siple Coast. At present day, a fast-flowing ice stream with a horizontal velocity of about 4 kilometers per year lies at the boundary between the retrograde and the prograde slopes of the Siple Coast (Mouginot et al., 2017).

410 At iteration 0 of the first timestep of the coupling method, the deformation in centimeters per year is assumed to be approximately zero. Using this deformation rate, grounded ice at the Siple Coast grows with up to 20 cm per year when using

this deformation (Figure S.3 in the supplementary materials). To analyze the effect of the coupling in detail, one area of 40 by 40 kilometers in the Siple Coast region is chosen around the latitude -84.7480 and longitude 219.2894.

During the first timestep, the ice thickness is increasing at every iteration, causing subsidence of the Earth's surface at every iteration. However, the rate of thickness and subsidence differs per iteration. The subsidence in this area increases at iteration 1 and 2 but decreases in iteration 3 (Table 1). The same trend can be seen at the whole Siple coast (Figures 6A-E). Following the change in deformation, the ice thickness increased more at iteration 2 compared to less increase at iteration 3 (Table 1). This trend for the whole Siple coast region is similar to the trend of the chosen area (Figures 6A-E).

**Table 1: Deformation rate and change in ice thickness for an area of 40 by 40 kilometers with latitude -84.7480 and longitude 219.2894 in the Siple Coast region, as a result of the coupled model using the 3D wet rheology.**

	Iteration 0	Iteration 1	Iteration 2	Iteration 3
Grounded ice thickness change [cm/year]		13	16	15
Deformation rate [cm/year]	$\pm 0$	-1	-1.5	-1.2

After three iterations, the mean deformation and ice thickness are computed over the last two iterations. The converged bedrock elevation at the chosen area subsides with 2 mm/year extra compared to iteration 1 (Figure 6G). The mean deformation over the last two iterations mainly differs from iteration 1 at the Siple Coast, the Ronne Ice Shelf, and several other locations along the grounding line (Figure 6G).

The mean change in ice thickness of 15.5 cm per year in the chosen area equals an ice growth of 770 meters in 5000 years. In the considered area, the ice thickness at the start of simulation, 120,000 years BP, was 757 meters so the ice sheet thickness doubled during the first timestep. In iteration 1, the computed change in ice thickness was 13 cm per year and thus underestimated the change in ice thickness. The mean ice thickness over the last two iterations mainly differs from iteration 1 at the Ross Ice Shelf, the Ronne Ice Shelf, and the mountain range in between (Figure 6H).

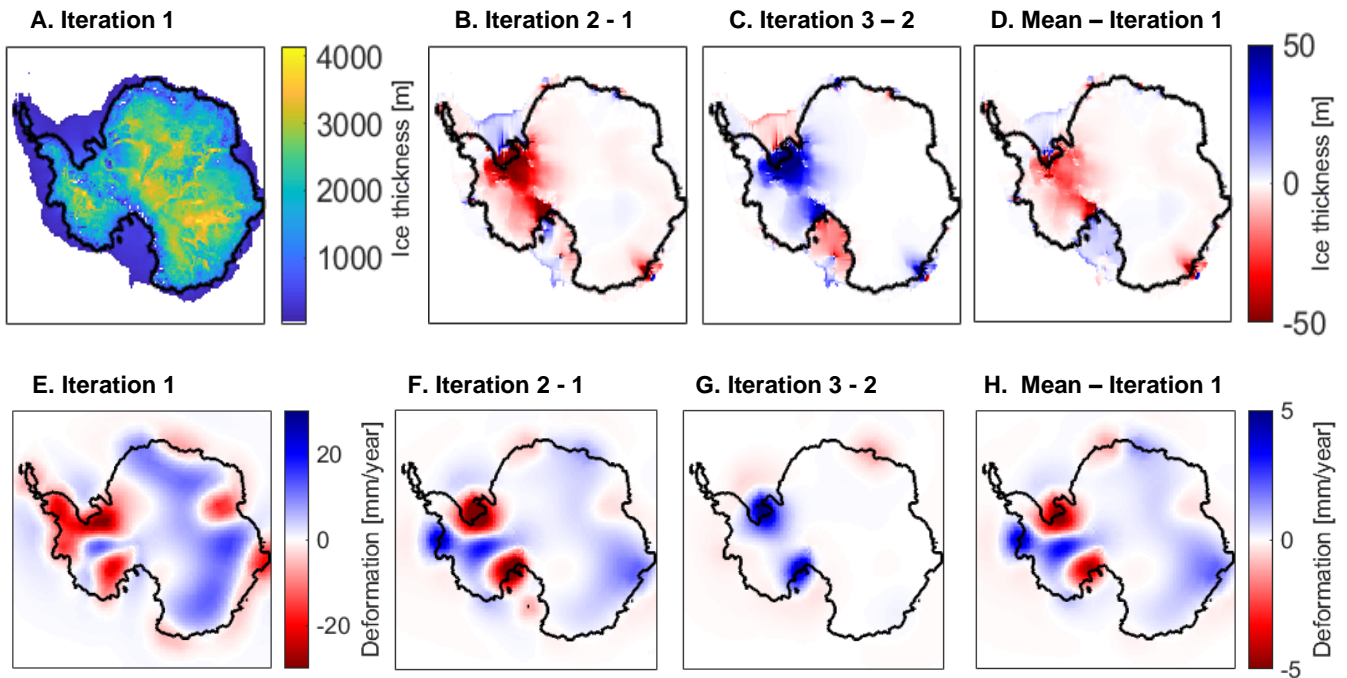


**Figure 6: Iterative process of timestep 1, 120,000 to 115,000 years BP, using the wet 3D rheology with a grainsize of 10 mm. Figures A-D show the ice thickness at 115,000 years BP where Figures B and C show the difference ice thickness of the corresponding iteration with the iteration before. Figures E-H show the deformation rate when applying the load shown in Figures A-C, where Figures F and G show the deformation difference of the corresponding iteration with the iteration before.**



During the first timestep, ice thickness is mostly increasing around the grounding line. Consequently, the grounding line is moving outward over time with a maximum of approximately 80 kilometers. Since the ice thickness increase was underestimated in the first iteration, the grounding line at the converged iteration differs with approximately 60 kilometers compared to iteration 1.

Although deformation and grounded ice thickness influence each other directly, also the ice shelf thickness changes per iteration (Figures 6D-H). Since calving occurs when the ice shelf thickness equals 200 meters, the calving line is also influenced by the coupling process. When grounded ice increased less compared to the former iteration, the ice shelf is thicker at the end of the timestep and the calving line position more outward. On the other hand, when grounded ice increased more compared to the former iteration, the ice shelf is thinner at the end of the timestep.

Similar effects can be observed when using the 1D and the 3D dry rheologies (Figure S.4 and S.5 in the supplementary material). For all three tests, the timestep results in an increased subsidence rate at the Ross Ice Shelf and the Ronne Ice Shelf compared to iteration 1. However, the deformation rate is lower for the 1D and dry 3D rheologies compared to the wet 3D rheology. Especially the number of iterations needed to reach convergence differs per rheology that is used. When simulating the full glacial cycle using a 1D rheology, two to three iterations are required per timestep to meet the convergence criterium. The first timestep using the 1D rheology is already converged with a difference smaller than 2 mm per year after two iterations. The dry 3D rheology converges after 3 iterations because the difference between iteration two and three is smaller than 2 mm per year. The wet 3D rheology does not convergence within 3 iterations at the Ross Ice Shelf and the Ronne Ice Shelf (Figure 6E). The required amount of iterations depends on the change in ice thickness within the timestep, which vary when using different rheologies. The required amount of iterations increases when lower viscosities are assigned to certain regions because the change in ice thickness increases for a changing viscosity.

Since the iterations do not perfectly convergence to zero, an uncertainty is introduced at every timestep. The uncertainty accumulates over time and reveals certain regions where the deformation rate is too high or the mantle viscosity too low to reach convergence to zero at every timestep. The accumulated convergence uncertainty of the coupled model using a 1D rheology is calculated for two time periods from 120 000 years to 20 000 years BP and from 20 000 years BP to modern date. The uncertainty of the convergence method in the first 100 000 years is concentrated to four regions: the Weddell sea embayment, the Ross sea embayment and, to a lesser extent, the peninsula and the Lambert Ice Shelf in East Antarctica (Figure 7A).

The uncertainty is maximum 8 mm per year in the first period towards LGM (Figure 7A), and maximum 4 millimeter per year in the period from LGM to modern date (Figure 7B). The deformation in the areas where the uncertainty is highest is mostly 1 to 2 cm per year. During the last period, the uncertainty extends a little further from the Weddell sea embayment towards East Antarctica along the grounding line. The uncertainty never exceeds 1 mm per year per timestep. However, the cumulative uncertainty at modern date goes up to 8 mm per year for certain areas of the Ross Ice Shelf and the Ronne Ice Shelf and several ice shelves of the East Antarctic Ice Sheet (Figure 7C). Considering the higher deformation rates at these regions, the accumulated uncertainty is acceptable but not neglectable.

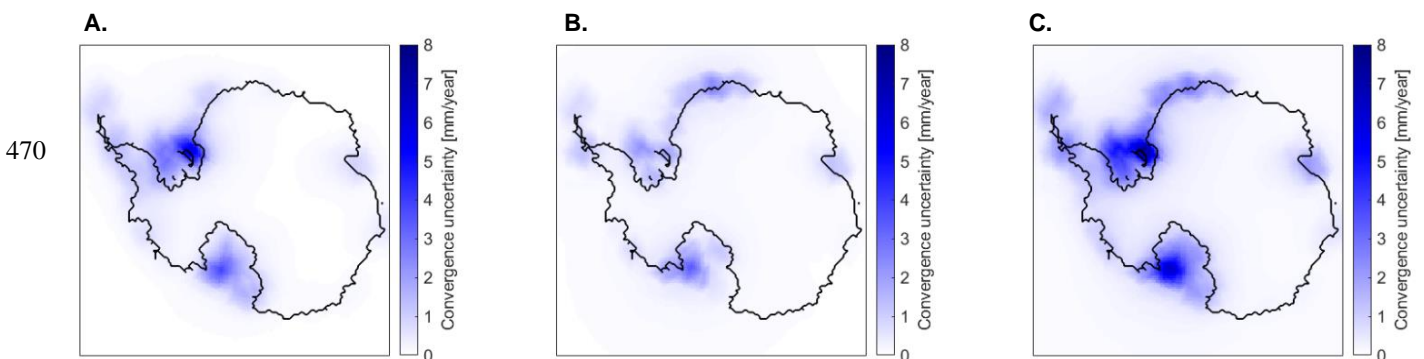


**Figure 7: A) Accumulated convergence uncertainty at Last Glacial Maximum B) Added convergence uncertainty during the period 20 000 years BP to modern date. C) Accumulated convergence uncertainty at modern date.**

#### 4. Discussion

The coupled model developed for this study allows to study the feedback loops between 3D GIA and ice sheet evolution at every chosen time step between 120,000 years BP and present day. The full glacial cycle is simulated using the coupled model with a 1D rheology. Since LGM, the results of the 1D coupled model show a steady uplift around the grounding line, the Ross Ice Shelf and the Ronne Ice Shelf up to  $15 \pm 3$  mm/year and a steady subduction in East Antarctica of about  $3 \pm 0$  mm/year. To better understand the results of the full glacial cycle, the first 5000 years of the simulation, from 120,000 to 115,000 years BP, is analyzed in detail using the 3D coupled model. Differences in the results of the first timestep when using different rheologies can fully be assigned to the coupling effect because the initial conditions remain the same for each test.

##### 4.1 The influence of the GIA feedback effects on regional ice sheet dynamics

The importance of the effect of using a 3D rheology to simulate the ice sheet evolution depends on the rheological model that is used. A higher water content, smaller grain size and higher temperatures in the upper mantle lead to increasing deformation rates. It follows from the results that the increasing deformation rates lead to increasing changes in ice thickness for both 3D rheologies when compared to ice thickness using a 1D rheology. The deformation pattern is similar when using three different rheologies, but the magnitude differs. The results of this study emphasize the importance of using a realistic range of rheologies for the analyses of the local ice sheet evolution.

The results of all three tests using different rheologies show a decay in ice mass in East Antarctica between 120,000 years and 115,000 years before present. This leads to a decrease in normal stresses along the ice sheet and thus a decrease of horizontal velocities, ultimately leading to a decrease of ice transported to the ice shelves (de Boer et al., 2013). On the other hand, the results show subsidence of the Earth surface at the Ronne Ice Shelf and the Ross Ice Shelf. Based on the Marine Ice Sheet Instability (MISI) process, increased ice shelf melt and fast grounding line retreat can be expected due to a retrograde bedrock slope and an increasing sea level caused by subsidence (Schoof, 2007). However, this effect is not observed in this study when using the deformation following from the first iteration of the coupled model.

It is demonstrated for the Ross Sea embayment that an increased subsidence in combination with a prograde bedrock slope does not necessarily result in Marine Ice Sheet Instability. This could be explained by increasing horizontal velocities. Due to the uplift at higher ice sheet surface elevations, the subsidence at lower elevations and an increasing stress in the ice sheet caused by an increasing ice mass, horizontal velocities of the ice sheet increase. This leads to a thickening ice sheet around the grounding line due to buttressing from the Ross Ice Shelf (Gagliardini et al., 2010).

Opposed to what was found in the first iteration, the MISI effect can be observed in the second iteration. The increased subsidence causes the sea level to rise fast enough to increase sub shelf melt from the ocean. Consequently, buttressing is decreased and the ice sheet thinnens. In the next iteration, the feedback effect is observed where the thinning ice sheet, and thus a decreasing ice mass, leads to a decrease in subsidence.

After convergence, subsidence and uplift areas are both increased compared to iteration 1. The maximum difference between the uncoupled deformation (iteration 1) and the coupled deformation (average between the last two iterations) for the period 120,000 to 115,000 years BP is 3 to 8 mm per year, depending on the viscosity of the upper mantle. Furthermore, the GIA feedback effect enhances deformation and ice dynamic processes at high elevations in East Antarctica and around fast flowing ice sheets like the Ronne Ice Shelf, the Ross Ice Shelf, and the Amery Ice Shelf. The GIA feedback effect weakens the deformation signal at the embayment's of the Bellinghausen, Lazarev, Riiser-Larsen, and Mawson seas.

Several studies emphasize the importance of accurate grounding line migration simulations on sea level rise projections and the simulation of the Antarctic Collapse (Gomez et al., 2010; Hay et al., 2017; Larour et al., 2019). A thickening ice sheet will drive the grounding line outward up to 200 kilometers. It can be concluded from the results that a relatively small change of tens of kilometers of the grounding line position over time, compared to the total area of Antarctica, results in a high increase of ice load over time. Since the change in ice sheet thickness is enhanced by the coupling effect, the grounding and calving

line migration is highly influenced by the feedback effects, emphasizing the importance of simulating the GIA feedback effect.

520 This study shows that the 3D GIA feedback effect should be considered when computing ice dynamics between the grounded ice sheet and the ice shelf to obtain more realistic results.

When simulating the ice sheet evolution with timesteps of 5000 years using a range of realistic rheologies, the coupled model is not capable of reaching a convergence of zero at each element of the models at regions where the change in ice thickness is high. This uncertainty should be considered since the regions where the change in ice thickness is high are more  
525 reactive to the GIA feedback effect. The uncertainty of the deformation rate does never exceed 1 mm per year per timestep for the tested rheologies, which is relatively low compared to the time averaged deformation rate itself. However, the model is using past results to simulate the new timestep. Therefore, uncertainties accumulate over time and become a significant percentage of the computed deformation rates that should be considered when analyzing the results.

High changes in grounded ice thickness over time occur often in some areas like the Ross Ice Shelf and the Ronne Ice  
530 Shelf, leading to a higher accumulated convergence uncertainty at present day. Since the change in ice thickness increases when using a rheological model with lower viscosities, also the convergence uncertainty increases when using 3D rheologies. Increasing the number of iterations by decreasing the convergence criterium of 2 mm deformation per year will lead to a smaller range of elements that alternate between a positive and negative value. It also decreases the range of deformation itself. However, convergence to zero cannot be reached solely by decreasing the convergence criterium. Decreasing the timestep or  
535 using relatively high viscosity values for the upper mantle does decrease the required number of iterations to reach convergence. This also decreases the area that does not convergence to zero, and thus decreases the uncertainty.

#### 4.3 Future approaches

The interactions between the ice sheet, ice shelf and the solid Earth in Antarctica are complex, dynamic, and challenging to model. Up till now, there was no model that includes GIA feedback effects on relatively short timescales of a thousand years  
540 in combination with 3D viscosities of the mantle under Antarctica. The highly varying viscosities of the mantle under Antarctica in combination with the importance of the GIA feedback effects asks for a new method that can include these effects on relatively short timescales. This study presents a new method to investigate 3D GIA feedback effects in detail at any chosen period during the last glacial cycle. The method is applied using ANICE and a 3D GIA FEM model. This led to the development of a fully coupled ice dynamic-3D GIA model with coupling timesteps of 1000 and 5000 years. The results of this study  
545 emphasize the importance of the 3D GIA feedback effects when simulating the evolution of the AIS. Therefore, the GIA feedback effects should be taken into account in future studies.

Including the Sea Level equation in the ice dynamic model allows to observe local changes in sea level (de Boer, 2014). This could be an important effect since subsidence of the bedrock leads to an increase of sea level and thus to an increase of ice shelf melt from below (Schoof, 2007). The effect of relative sea level on the evolution of the ice sheet using a coupled  
550 model is shown to be significant in Gomez et al. (2018). This effect is included in the coupled model used in this study but the change in sea level is not coupled to the ice dynamic, nor to the GIA model. The GIA model could be used to compute the geoid at the end of each timestep by using the sea level equation. Furthermore, local changes in sea level could be implemented in ANICE to include the effect of self-gravitation on the evolution of the ice sheet.

Deformation of the bedrock alters ice thickness and grounding line migration, dependent on the bedrock shape (Adhikari  
555 et al., 2019). Strong spatial variability in uplift rates, especially is West Antarctica and the Antarctic peninsula, imply a high variability in bedrock slope (Gomez et al., 2013; Konrad et al., 2013). Low resolution bounds of tens to hundreds of kilometers do not capture the complex bed topography of the ice streams of West Antarctica (Larour et al., 2019). However, the local differences in dynamics are observed in this study using the ice model on spatial scales of 40 by 40 kilometers and using the GIA model on spatial scales of 200 by 200 kilometers. These spatial scales are acceptable to study ice sheet evolution for the

560 whole AIS but higher resolution models are necessary to simulate an accurate grounding line migration patterns and to study local uplift rates and changes in the ice balance in detail for a small region.

The resolution of ANICE can easily be increased to 20 by 20 kilometers for the whole region. The 3D GIA model used in this study can also easily be increased in any chosen area to any chosen resolution, while maintaining a coarser global resolution. However, an increased resolution also increases the computation time up to several weeks compared to the currently  
565 used grid. It is recommended to accept the long computation time in order to obtain results on a high resolution. Detailed analysis of different areas can provide new insights on ice dynamics and its implications on climate change globally.

Another effect on local sea level could be sediment deposition. This is not accounted for in this study but could cause a systematic uplift of the Earth's surface (van der Wal & Ijpelaar, 2017). Detailed recommendations to improve the coupled model can be found in section D.2 of Appendix D.

570 Simulations of the full glacial cycle from 120,000 years BP till present day using a high-resolution grid and a laterally varying rheology are ready to start but these simulations are computationally expensive and take several weeks to finish. For this reason, these simulations are not performed here. However, simulations of the full glacial cycle using laterally varying rheologies provide realistic present-day uplift rates and changes in the mass balance of the AIS using an ice history that is consistent with a 3D Earth rheology. This allows a more detailed analysis of the 3D GIA feedback effects on long timescales,  
575 including long- and short-term deformation caused by GIA. This is particularly important to validate currently used uplift rates to correct GPS measurements for GIA. The simulations are not bounded to the Antarctic region. Since the GIA model and the ice dynamic model are both global models, the model can also be used to study the Greenland Ice Sheet.

## References

- A, G., Wahr, J., and Zhong, S.: Computations of the viscoelastic response of a 3-D compressible Earth to surface loading: an  
580 application to Glacial Isostatic Adjustment in Antarctica and Canada. *Geophysical Journal International*, 192, 557-572, doi:10.1093/gji/ggs030, 2013.
- Alley, R.B., Blankenship, D.D., Bentley, C.R., and Rooney, S.T.: Deformation of till beneath ice stream B, West Antarctica. *Nature*, 322, 57-59, doi:10.1038/322057a0, 1986.
- Atkinson, A., Siegel, V., Pakhomov, E., and Rothery, P.: Long-term decline in krill stock and increase in salps within the  
585 Southern Ocean. *Nature*, 432, 100-103, doi:10.1038/nature02996, 2004.
- Barletta, V.R., Bevis, M., Smith, B.E., ... and Smalley, R.: Observed rapid bedrock uplift in Amundsen Sea Embayment promotes ice-sheet stability. *Science*, 360, 1335-1339, doi:10.1126/science.aao1447, 2018.
- Barrett, P.J.: Antarctic Palaeoenvironment through Cenozoic Times. *Terra Antarctica*, 3, 103-109, 1996.
- Becker, T.W., and Boschi, L.: A comparison of tomographic and geodynamic mantle models. *Geochemistry, Geophysics, Geosystems*, 3, doi:10.1029/2001GC000168, 2002.  
590
- Bell, R.E., and Seroussi, H.: History, mass loss, structure, and dynamic behavior of the Antarctic Ice Sheet. *Science*, 367, 1321-1325, doi:10.1126/science.aaz5489, 2020.
- Berends, C.J., de Boer, B., and van de Wal, R.S.W.: Application of HadCM3@ Bristolv1. 0 simulations of paleoclimate as forcing for an ice-sheet model, ANICE2. 1: set-up and benchmark experiments. *Geoscientific Model Development*, 11,  
595 4657-4675, doi:10.5194/gmd-11-4657-2018, 2018.
- Bintanja, R., Van de Wal, R.S.W., and Oerlemans, J.: Global ice volume variations through the last glacial cycle simulated by a 3-D ice-dynamical model. *Quaternary International*, 95, 11-23, doi:10.1016/S1040-6182(02)00023-X, 2002.
- Bintanja, R., van de Wal, R., and Oerlemans, J.: Modelled atmospheric temperatures and global sea levels over the past million years. *Nature*, 437, 125-128, <https://doi.org/10.1038/nature03975>, 2005.

- 600 Bintanja, R., and van de Wal, R.: North American ice-sheet dynamics and the onset of 100,000-year glacial cycles. *Nature*, 454, 869–872, doi:10.1038/nature07158, 2008.
- Blank, B., Barletta, V., Hu, V., and van der Wal, W.: Evaluation of differences between 1D, 3D and 4D models in the Amundsen Sea Embayment Region by use of Finite Element Based GIA models. In preparation.
- Bradley, S.L., Reerink, T.J., van de Wal, R.S.W., and Helsen, M.M.: Simulation of the Greenland Ice Sheet over two glacial–  
605 interglacial cycles: investigating a sub-ice- shelf melt parameterization and relative sea level forcing in an ice-sheet–ice-shelf model, *Climate of the Past*, 14, 619–635, doi:10.5194/cp-14-619-2018, 2018.
- Bueler, E., and Brown, J.: Shallow shelf approximation as a “sliding law” in a thermomechanically coupled ice sheet model. *Journal of Geophysical Research: Earth Surface*, 114, F03008, doi:10.1029/2008JF001179, 2009.
- Bulthuis, K., Arnst, M., Sun, S., and Pattyn, F.: Uncertainty quantification of the multi-centennial response of the Antarctic  
610 ice sheet to climate change. *The Cryosphere*, 13, 1349-1380, doi:10.5194/tc-13-1349-2019, 2019.
- Chown, S.L., and Brooks, C.M.: The state and future of Antarctic environments in a global context. *Annual Review of Environment and Resources*, 44, 1-30, doi:10.1146/annurev-environ-101718-033236, 2019.
- Constable, A.J., Melbourne-Thomas, J., Corney, S.P., ... and Davidson, A.T.: Climate change and Southern Ocean ecosystems I: how changes in physical habitats directly affect marine biota. *Global change biology*, 20, 3004-3025,  
615 doi:10.1111/gcb.12623, 2014.
- Creys, T.T., Ferraccioli, F., Bell, R.E., ... and Finn, C.: Freezing of ridges and water networks preserves the Gamburtsev Subglacial Mountains for millions of years. *Geophysical Research Letters*, 41, 8114-8122, doi:10.1002/2014GL061491, 2014.
- de Boer, B., van de Wal, R.S.W., Lourens, L.J., Bintanja, R., and Reerink, T.J.: A continuous simulation of global ice volume  
620 over the past 1 million years with 3-D ice-sheet models. *Climate Dynamics*, 41, 1365–1384, doi:10.1007/s00382-012-1562-2, 2013.
- de Boer, B., Stocchi, P., and van de Wal, R.: A fully coupled 3-D ice-sheet-sea-level model: algorithm and applications. *Geoscientific Model Development*, 7, 2141-2156, doi:10.5194/gmd-7-2141-2014, 2014.
- de Boer, B., Dolan, A.M., Bernales, J., Gasson, E., Golledge, N.R., Sutter, J., Huybrechts, P., Lohmann, G., Rogozhina, I.,  
625 Abe-Ouchi, A., Saito, F., and van de Wal, R.S.W.: Simulating the Antarctic Ice Sheet in the late-Pliocene warm period: PLISMIP-ANT, an ice-sheet model intercomparison project. *The Cryosphere*, 9, 881–903, doi:10.5194/tc-9-881-2015, 2015.
- de Boer, B., Stocchi, P., Whitehouse, P.L., and van de Wal, R.S.: Current state and future perspectives on coupled ice-sheet–sea-level modelling. *Quaternary Science Reviews*, 169, 13-28, doi:10.1016/j.quascirev.2017.05.013, 2017.
- 630 DeConto, R.M., and Pollard, D.: Contribution of Antarctica to past and future sea-level rise. *Nature*, 531, 591-597, doi:10.1038/nature17145, 2016.
- Fretwell, P., Pritchard, H.D., Vaughan, D.G., ... and Catania, G.: Bedmap2: improved ice bed, surface and thickness datasets for Antarctica. *The Cryosphere*, 7, 375-393, doi:10.5194/tc-7-375-2013, 2013.
- Fricker, H.A., Scambos, T., Bindschadler, R., and Padman, L.: An active subglacial water system in West Antarctica mapped  
635 from space. *Science*, 315(5818), 1544-1548, doi:10.1126/science.1136897, 2007.
- Gagliardini, O., Durand, G., Zwinger, T., Hindmarsh, R.C.A., and Le Meur, E.: Coupling of ice-shelf melting and buttressing is a key process in ice-sheets dynamics. *Geophysical Research Letters*, 37, doi:10.1029/2010GL043334, 2010.
- Goes, S., Govers, R., and Vacher, A.P.: Shallow mantle temperatures under Europe from P and S wave tomography. *Journal of Geophysical Research: Solid Earth*, 105, 11153-11169, doi:10.1029/1999JB900300, 2002.
- 640 Goldberg, D., Holland, D.M., and Schoof, C.: Grounding line movement and ice shelf buttressing in marine ice sheets. *Journal of Geophysical Research: Earth Surface*, 114, doi:10.1029/2008JF001227, 2009.

- Gomez, N., Mitrovica, J.X., Tamisiea, M.E., and Clark, P.U.: A new projection of sea level change in response to collapse of marine sectors of the Antarctic Ice Sheet. *Geophysical Journal International*, 180, 623-634, doi:10.1111/j.1365-246X.2009.04419.x, 2010.
- 645 Gomez, N., Latychev, K., and Pollard, D.: A Coupled Ice Sheet–Sea Level Model Incorporating 3D Earth Structure: Variations in Antarctica during the Last Deglacial Retreat. *Journal of Climate*, 31, 4041–4054, doi:10.1175/JCLI-D-17-0352.1, 2018.
- Gordon, R.B.: Diffusion creep in the Earth's mantle. *Journal of Geophysical Research*, 70, 2413-2418, doi:10.1029/JZ070i010p02413, 1965.
- Hay, C.C., Lau, H.C., Gomez, N., ... and Wiens, D.A.: Sea level fingerprints in a region of complex Earth structure: The case of WAIS. *Journal of Climate*, 30, 1881-1892, doi:10.1175/JCLI-D-16-0388.1, 2017.
- 650 Heeszel, D.S., Wiens, D.A., Anandakrishnan, S., ... and Winberry, J.P.: Upper mantle structure of central and West Antarctica from array analysis of Rayleigh wave phase velocities. *Journal of Geophysical Research: Solid Earth*, 121, 1758-1775, doi:10.1002/2015JB012616, 2016.
- Hibbitt, D., Karlsson, B. and Sorensen, P.: *Getting Started with ABAQUS, Version (6.14)*, Hibbitt, Karlsson & Sorensen, Inc, 655 2016.
- Hindell, M.A., Reisinger, R.R., Ropert-Coudert, Y., ... and Lea, M.A.: Tracking of marine predators to protect Southern Ocean ecosystems. *Nature*, 580, 87-92, doi:10.1038/s41586-020-2126-y, 2020.
- Hirth, G., and Kohlstedt, D.: Rheology of the upper mantle and the mantle wedge: A view from the experimentalists. *Geophysical Monograph-American Geophysical Union*, 138, 83-106, doi:10.1029/138GM06, 2003.
- 660 Hu, H., van der Wal, W., and Vermeersen, L.L.A.: A numerical method for reorientation of rotating tidally deformed viscoelastic bodies. *Journal of Geophysical Research: Planets*, 122, 228-248, doi:10.1002/2016JE005114, 2017.
- Karato, S.I., Paterson, M.S., and FitzGerald, J.D.: Rheology of synthetic olivine aggregates: influence of grain size and water. *Journal of Geophysical Research: Solid Earth*, 91, 8151-8176, doi:10.1029/JB091iB08p08151, 1986.
- Karato, S.I., Jung, H., Katayama, I., and Skemer, P.: Geodynamic significance of seismic anisotropy of the upper mantle: new 665 insights from laboratory studies. *Annual Review of Earth and Planetary Sciences*, 36, 59-95, doi:10.1146/annurev.Earth.36.031207.124120, 2008.
- Kaufmann, G., Wu, P., and Ivins, E.R.: Lateral viscosity variations beneath Antarctica and their implications on regional rebound motions and seismotectonics. *Journal of Geodynamics*, 39, 165-181, doi:10.1016/j.jog.2004.08.009, 2005.
- Kendall, R.A., Mitrovica, J.X., and Milne, G.A.: On post-glacial sea level–II. Numerical formulation and comparative results 670 on spherically symmetric models. *Geophysical Journal International*, 161, 679-706, doi:10.1111/j.1365-246X.2005.02553.x, 2005.
- Konrad, H., Sasgen, I., Pollard, D., and Klemann, V.: Potential of the solid-Earth response for limiting long-term West Antarctic Ice Sheet retreat in a warming climate. *Earth and Planetary Science Letters*, 432, 254-264, doi:10.1016/j.epsl.2015.10.008, 2015.
- 675 Larour, E., Seroussi, H., Adhikari, S., Ivins, E., Caron, L., Morlighem, M., and Schlegel, N.: Slowdown in Antarctic mass loss from solid Earth and sea-level feedbacks. *Science*, 364, doi:10.1126/science.aav7908, 2019.
- Laskar, J., Robutel, P., Joutel, F., Gastineau, M., Correia, A.C.M., and Levrard, B.: A long-term numerical solution for the insolation quantities of the Earth. *Astronomy & Astrophysics*, 428, 261-285, doi:10.1051/0004-6361:20041335, 2004.
- Latychev, K., Mitrovica, J.X., Tromp, J., Tamisiea, M.E., Komatitsch, D., and Christara, C.C.: Glacial isostatic adjustment on 680 3-D Earth models: a finite-volume formulation. *Geophysical Journal International*, 161, 421-444, doi:10.1111/j.1365-246X.2005.02536.x, 2005.
- Le Meur, E., and Huybrechts, P.: A comparison of different ways of dealing with isostasy: examples from modelling the Antarctic Ice Sheet during the last glacial cycle. *Annals of Glaciology*, 23, 309-317, doi:10.3189/S0260305500013586, 1996.

- 685 Maris, M.N.A., de Boer, B., Ligtenberg, S.R.M., Crucifix, M., van de Berg, W.J., and Oerlemans, J.: Modelling the evolution of the Antarctic Ice Sheet since the last interglacial, *The Cryosphere*, 8, 1347–1360, doi:10.5194/tc-8-1347-2014, 2014.
- Martin, M.A., Winkelmann, R., Haseloff, M., Albrecht, T., Bueller, E., Khroulev, C., and Levermann, A.: The Potsdam Parallel Ice Sheet Model (PISM-PIK)-part 2: dynamic equilibrium simulation of the Antarctic Ice Sheet. *The Cryosphere*, 5, 3, 727-740, doi:10.5194/tc-5-727-2011, 2011.
- 690 Meredith, M., Sommerkorn, M., Cassotta, S., ... Schuur, E.A.G.: Chapter 3: Polar Regions. IPCC SR Ocean and Cryosphere, 2019.
- Morland, L.W., and Johnson, I.R.: Steady motion of ice sheets. *Journal of Glaciology*, 25, 229–246, doi:10.3189/S0022143000010467, 1980.
- Morland, L.W.: Unconfined ice-shelf flow. *Dynamics of the West Antarctic Ice Sheet*, 99–116, doi:10.1007/978-94-0093745-1\_6, 1987.
- 695 Morlighem, M., Rignot, E., Binder, T., ... and Young, D.: Deep glacial troughs and stabilizing ridges unveiled beneath the margins of the Antarctic Ice Sheet. *Nature Geoscience*. 13, 132–137, doi:10.1038/s41561-019-0510-8, 2020.
- Mouginot, J., Rignot, E., Scheuchl, B., and Millan, R.: Comprehensive annual ice sheet velocity mapping using Landsat-8, Sentinel-1, and RADARSAT-2 data. *Remote Sensing*, 9, 364, doi:10.3390/rs9040364, 2017.
- 700 Muis, S., Apecechea, M.I., Dullaart, J., ... and Verlaan, M.: A High-Resolution Global Dataset of Extreme Sea Levels, Tides, and Storm Surges, Including Future Projections. *Frontiers in Marine Science*, 7, 263, doi:10.3389/fmars.2020.00263, 2020
- Naish, T., Powell, R., Levy, R., ... and Carter, L.: Obliquity-paced Pliocene West Antarctic Ice Sheet oscillations. *Nature*, 458, 322-328, doi:10.1038/nature07867, 2009.
- Nield, G.A., Barletta, V.R., Bordoni, A., ... and Berthier, E.: Rapid bedrock uplift in the Antarctic Peninsula explained by viscoelastic response to recent ice unloading. *Earth and Planetary Science Letters*, 397, 32-41, doi:10.1016/j.epsl.2014.04.019, 2014.
- 705 Nield, G.A., Whitehouse, P.L., van der Wal, W., Blank, B., O'Donnell, J.P., and Stuart, G.W.: The impact of lateral variations in lithospheric thickness on glacial isostatic adjustment in West Antarctica. *Geophysical Journal International*, 214, 811-824, doi:10.1093/gji/ggy158, 2018.
- 710 Oppenheimer, M., Glavovic, B.C., Hinkel, J., ... and Sebesvari, Z.: Sea Level Rise and Implications for Low-Lying Islands, Coasts and Communities. IPCC Special Report on the Ocean and Cryosphere in a Changing Climate [H.-O. Pörtner, D.C. Roberts, V. Masson-Delmotte, P. Zhai, M. Tignor, E. Poloczanska, K. Mintenbeck, A. Alegría, M. Nicolai, A. Okem, J. Petzold, B. Rama, N.M. Weyer (eds.)]. In press, 2019.
- Oude Egbrink, D.F.: Modelling the Last Glacial Ice Sheet on Antarctica with Laterally Varying Relaxation Time. Master Thesis, Delft University of Technology, 2017.
- 715 Pattyn, F., and Morlighem, M.: The uncertain future of the Antarctic Ice Sheet. *Science*, 367, 1331-1335, doi:10.1126/science.aaz5487, 2020.
- Petit, J.R., Jouzel, J., Raynaud, D., ... and Delmotte, M.: Climate and atmospheric history of the past 420,000 years from the Vostok ice core, Antarctica. *Nature*, 399, 429, doi:10.1038/20859, 1999.
- 720 Pollard, D., and DeConto, R.: Modelling West Antarctic Ice Sheet growth and collapse through the past five million years. *Nature*, 458, 329–332, doi:10.1038/nature07809, 2009.
- Pollard, D., Gomez, N., and DeConto, R.M.: Variations of the Antarctic Ice Sheet in a coupled ice sheet-Earth-sea level model: sensitivity to viscoelastic Earth properties. *Journal of Geophysical Research: Earth Surface*, 122, 2124-2138, doi:10.1002/2017JF004371, 2017.
- 725 Ranalli, G.: *Rheology of the Earth*. Springer Science & Business Media, ISBN:0412546701, 1995.

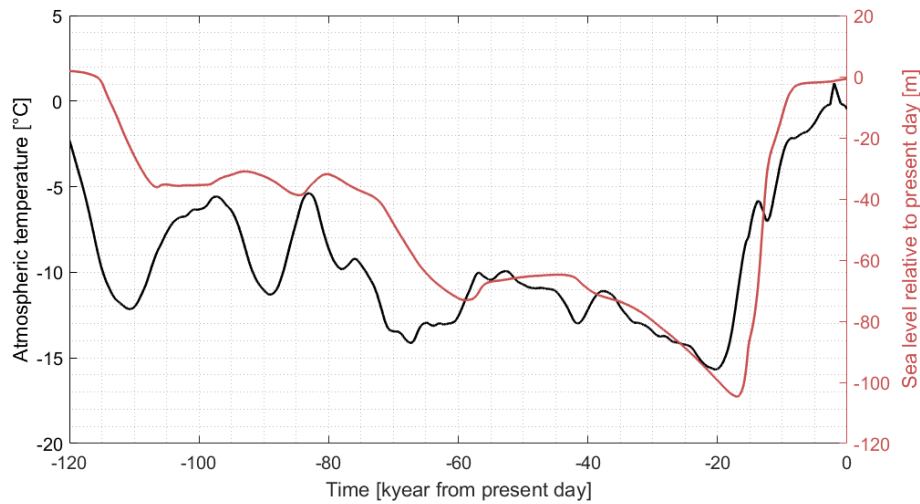
- Reerink, T.J., Van De Berg, W.J., and Van De Wal, R.S.: OBLIMAP 2.0: a fast climate model-ice sheet model coupler including online embeddable mapping routines. *Geoscientific Model Development*, 9, 4111-4132, doi:10.5194/gmd-9-4111-2016, 2016.
- Schaeffer, A.J., and Lebedev, S.: Global shear speed structure of the upper mantle and transition zone. *Geophysical Journal International*, 194, 417-449, doi:10.1093/gji/ggt095, 2013.
- 730 Schoof, C.: Ice sheet grounding line dynamics: Steady states, stability, and hysteresis. *Journal of Geophysical Research: Earth Surface*, 112, doi:10.1029/2006JF000664, 2007.
- Seroussi, H., Nowicki, S., Payne, A.J., ... and Calov, R.: ISMIP6 Antarctica: a multi-model ensemble of the Antarctic Ice Sheet evolution over the 21st century, *The Cryosphere Discuss.*, doi:10.5194/tc-2aqiuzazaaaa019-324, in review, 2020.
- 735 Shepherd, A., Ivins, E., Rignot, E., ... and Nowicki, S.: Mass balance of the Antarctic Ice Sheet from 1992 to 2017. *Nature*, 558, 219-222, doi:10.1038/s41586-018-0179-y, 2018.
- Smith, B., Fricker, H.A., Gardner, A.S., ..., and H.J. Zwally.: Pervasive ice sheet mass loss reflects competing ocean and atmosphere processes. *Science*, doi:10.1126/science.aaz5845, 2020.
- Stark, J.S., Raymond, T., Deppeler, S.L., and Morrison, A.K.: Antarctic Seas. In *World Seas: An Environmental Evaluation*. Academic Press, 1, 1-44, doi:10.1016/B978-0-12-805068-2.00002-4, 2019.
- 740 Tromp, J., and Mitrovica, J.X.: Surface loading of a viscoelastic earth—I. General theory. *Geophysical Journal International*, 137, 3, 847–855, doi:10.1046/j.1365-246x.1999.00838.x, 1999.
- Turney, C.S., Fogwill, C.J., Golledge, N.R., ... and Ramsey, C.B.: Early Last Interglacial ocean warming drove substantial ice mass loss from Antarctica. *Proceedings of the National Academy of Sciences*, 117, 3996-4006, doi:10.1073/pnas.1902469117, 2020.
- 745 van der Wal, W., Barnhoorn, A., Stocchi, P., Gradmann, S., Wu, P., Drury, M., and Vermeersen, B.: Glacial isostatic adjustment model with composite 3-D Earth rheology for Fennoscandia. *Geophysical Journal International*, 194, 61-77, doi:10.1093/gji/ggt099, 2013.
- van der Wal, W., Whitehouse, P.L., and Schrama, E.J.O.: Effect of GIA models with 3D composite mantle viscosity on GRACE mass balance estimates for Antarctica. *Earth and Planetary Science Letters*, 414, 134–143, doi:10.1016/j.epsl.2015.01.001, 2015.
- 750 van der Wal, W., and IJpelaar, T.: The effect of sediment loading in Fennoscandia and the Barents Sea during the last glacial cycle on glacial isostatic adjustment observations. *Solid Earth*, 8, 955-968, doi:10.5194/se-8-955-2017, 2017.
- Weerdesteijn, M.F.M.: The implementation of glaciation-induced rotational behavior of the Earth in a numerical model. Master Thesis, Delft University of Technology, 2019.
- 755 Wessel, P., and Becker, J.M.: Interpolation using a generalized Green's function for a spherical surface spline in tension. *Geophysical Journal International*, 174, 21-28, doi:10.1111/j.1365-246X.2008.03829.x, 2008.
- Whitehouse, P: Glacial isostatic adjustment and sea-level change. State of the art report (No. SKB-TR--09-11). Swedish Nuclear Fuel and Waste Management Co, 2009.
- 760 Whitehouse, P.L., Bentley, M.J., Milne, G.A., King, M.A., and Thomas, I.D.: A new glacial isostatic adjustment model for Antarctica: calibrated and tested using observations of relative sea-level change and present-day uplift rates. *Geophysical Journal International*, 190, 1464-1482, doi:10.1111/j.1365-246X.2012.05557.x, 2012.
- Whitehouse, P.L., Gomez, N., King, M.A., and Wiens, D.A.: Solid Earth change and the evolution of the Antarctic Ice Sheet. *Nature communications*, 10, 1-14, doi:10.1038/s41467-018-08068-y, 2019.
- 765 Winkelmann, R., Martin, M.A., Haseloff, M., Albrecht, T., Bueller, E., Khroulev, C., and Levermann, A.: The Potsdam parallel ice sheet model (PISM-PIK)-Part 1: Model description. *The Cryosphere*, 5, 715-726, doi:10.5194/tc-5-715-2011, 2011.



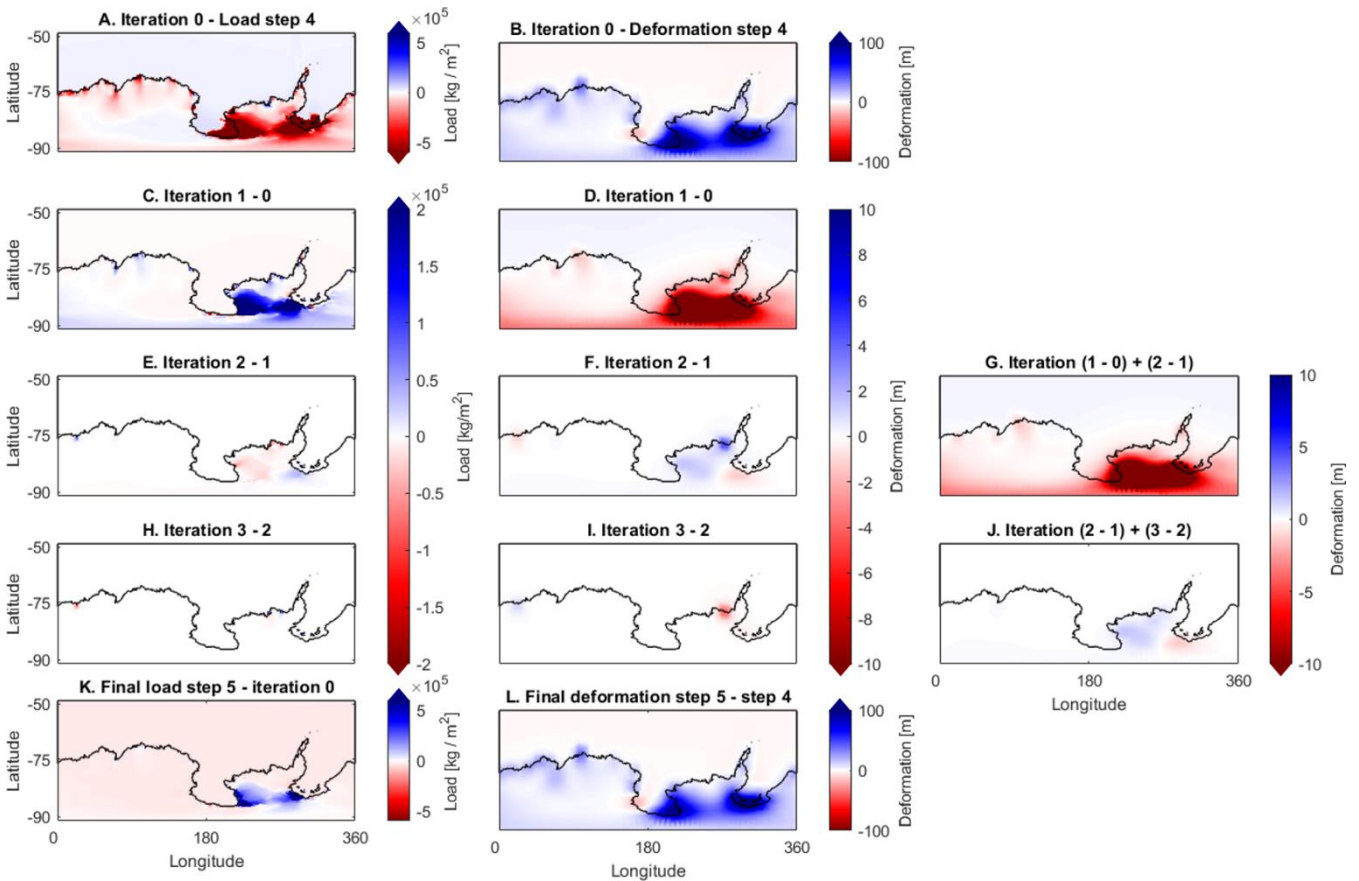
Wolstencroft, M., King, M.A., Whitehouse, P.L., ..., and Gunter, B.C.: Uplift rates from a new high-density GPS network in Palmer Land indicate significant late Holocene ice loss in the southwestern Weddell Sea. *Geophysical Journal International*, 203, 1, 737–754, doi:10.1093/gji/ggv327, 2015.

770 Wu, P.: Using commercial finite element packages for the study of Earth deformations, sea levels and the state of stress. *Geophysical Journal International*, 158, 2, 401–408, doi:10.1111/j.1365-246X.2004.02338.x, 2004.

Supplemental material

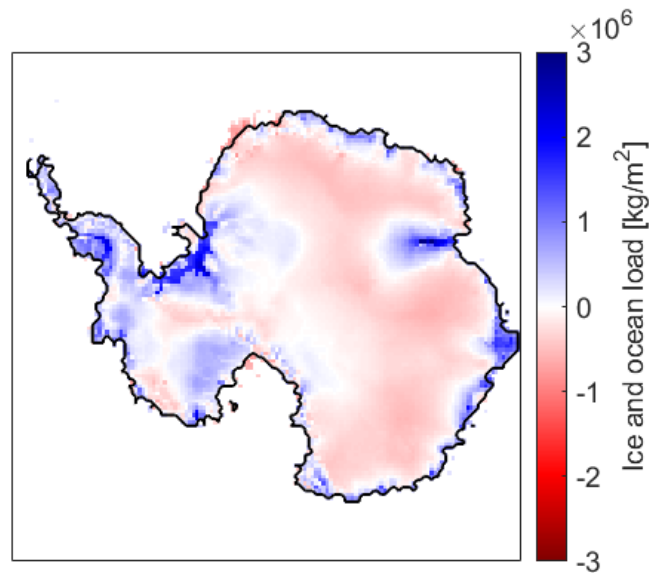


775 **Figure S.1: Atmospheric temperature (black) and eustatic sea level relative to present day (red). Both are shown over time, starting 120 000 years BP.**



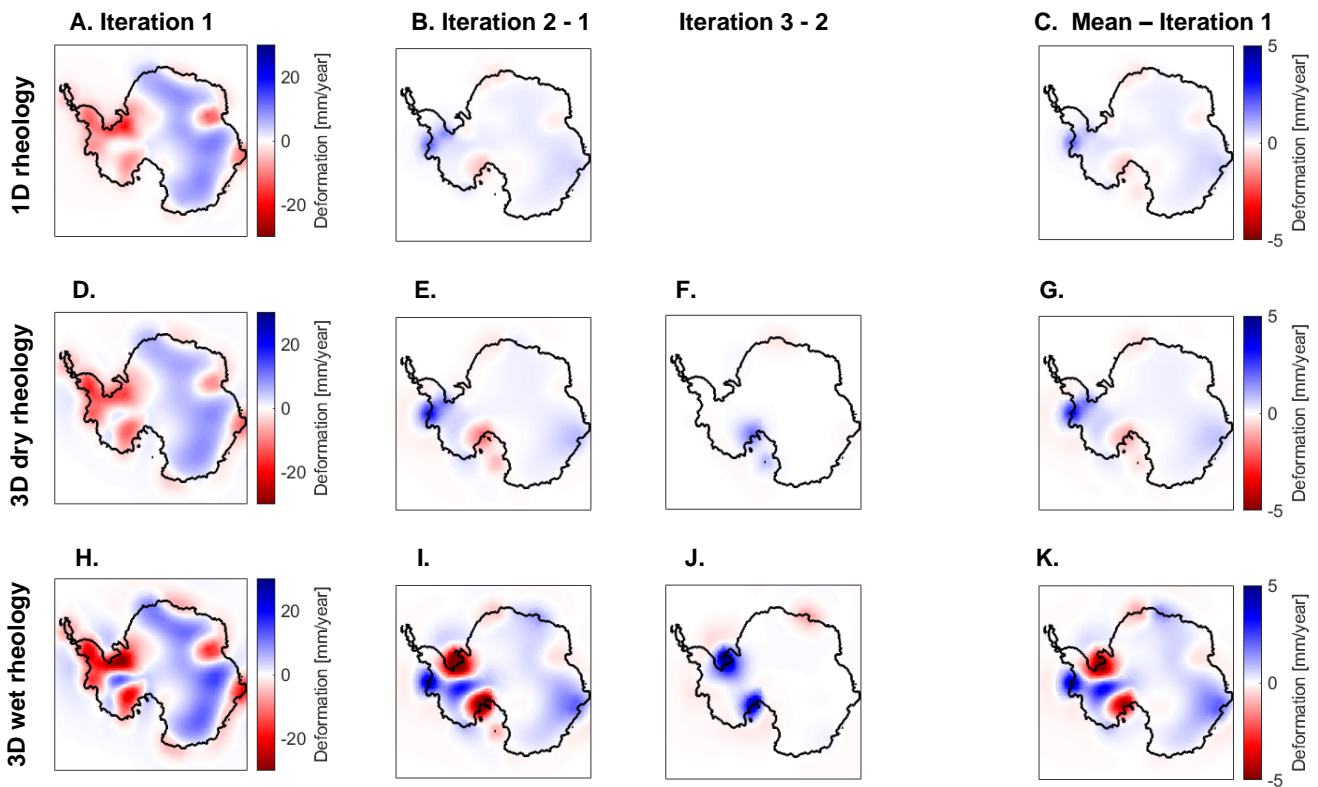
780 **Figure S.2: Overview of the iterative process of the coupling method for timestep 5; 95 000 till 90 000 years before present (BP).** Antarctica is shown on an equidistant, Asia centred, grid at all longitudes. The black line is the grounding line at 90 000 years BP of iteration 3 and is the same in every Figure to allow for comparison. A) Relative sea level and ice thickness in meters multiplied by the assumed density of water and ice respectively computed by ANICE. The difference is shown between the final load at step 4 and the first iteration of step 5. The input for iteration 0 is the final deformation of step 4. B) Computed deformation by the GIA model using the load from Figure A as input. The difference is shown between iteration 0 of step 5 and the final deformation of step. This shows the effect of the change in load shown in Figure A. C-G) Difference in load and deformation with former iteration. G) Addition of Figures D and F. H-I) Difference in load and deformation with former iteration. J) Addition of Figures F and I. The difference is everywhere smaller than 10 meters and the convergence criterium has been met. K) Difference between final load of step 5 and the load from iteration 0. The final load of step 5 is calculated by taking the average at each grid cell from iterations 2 and 3. L) Difference of final deformation between timestep 4 and 5. The final load of step 5 is computed by ANICE using the final deformation of step 5 as input. Figures K and L show the total effect of the full iteration process.

785



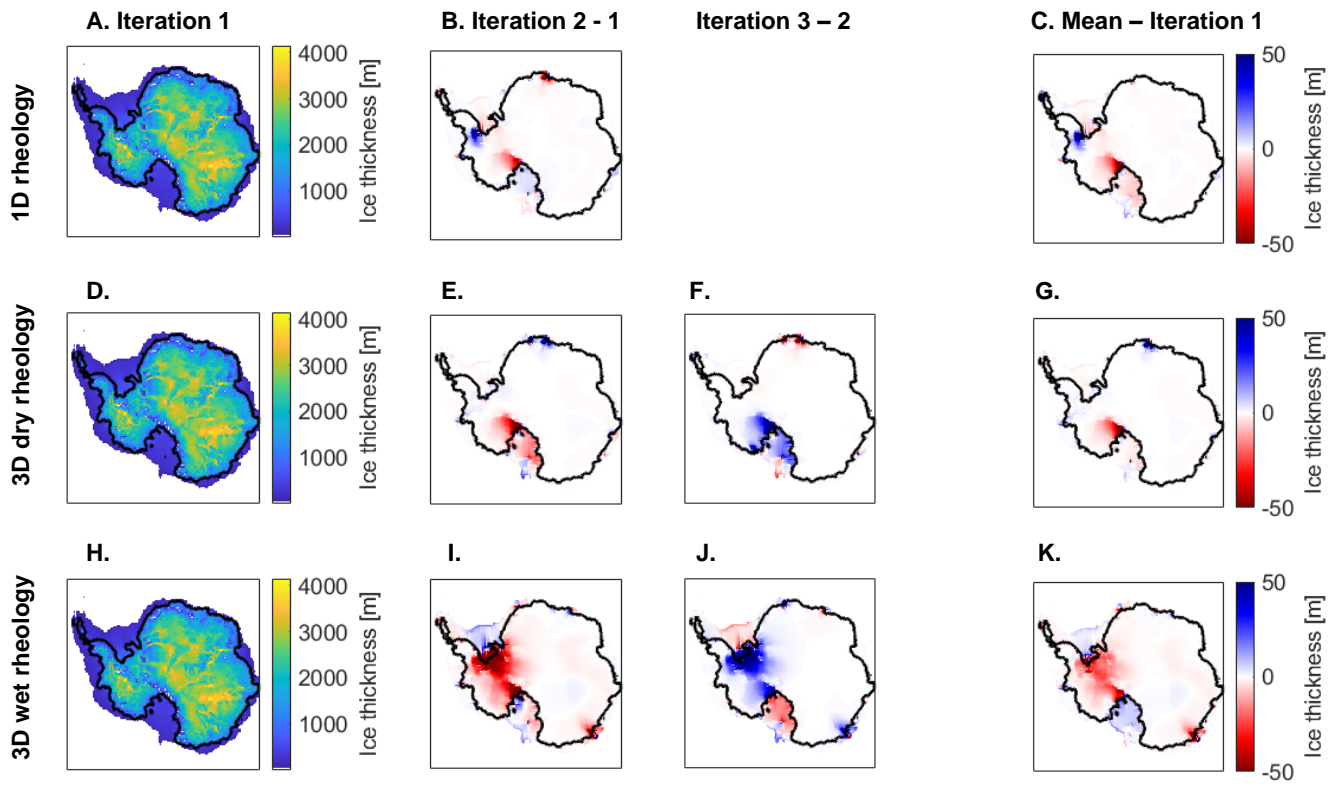
790

Figure S.3: The assumed change in ice and ocean load for the period 120,000 years BP to 115,000 years BP, following from a deformation that is close to zero.



795

Figure S.4: Iteration process of timestep 1, 120,000 to 115,000 years BP, using three different rheologies. For the three different rheologies, the same initial load is applied at iteration 1. Figures A-C show the deformation rate for the 1D rheology, where Figures B and C show the difference in deformation of the average of the last two iterations with iteration 1. Figures D-G show the deformation rate for the 3D dry rheology with a grain size of 4 mm. Figures H-K show the deformation rate for the 3D wet rheology with a grain size of 10 mm.



800

Figure S.5: Iteration process of timestep 1, 120,000 to 115,000 years BP, using three different rheologies. For the three different rheologies, the obtained deformation from Figure S.3 is used at iteration 1. Figures A-C show the ice thickness for the 1D rheology, where Figures B and C show the difference in ice thickness of that iteration with iteration 1. Figures D-G show the ice thickness for the 3D dry rheology with a grain size of 4 mm. Figures H-K show ice thickness for the 3D wet rheology with a grain size of 10 mm.

# 3

## Conclusions

The goal of this study is to present a new method to fully couple an ice- and 3D GIA model at timescales of 1000 to 5000 years for the AIS. In this section, an overview is provided of the main conclusions that can be drawn from this study.

### *How can the GIA FEM model and ANICE be coupled?*

Up to now, no method exists for the coupling of a 3D GIA model to an ice-sheet-shelf model on relatively short timescales of thousands of years. Therefore, there was a need for a new method to study the effect of 3D mantle viscosity on the Antarctic Ice Sheet growth during the last glacial cycle.

To approach the continuous interaction between GIA and ice sheet dynamics, a period of 5000 years is considered as coupling time step. However, to compute GIA over this period, the load of the ice should be known and to compute changes in ice sheet characteristics and grounding line migration, the deformation of the Earth's surface should also be known. An iterative process can be used to find an equilibrium state at each timestep.

To decide when the equilibrium state has been reached, a convergence criterium must be constructed. Two different criteria were tested, resulting in the choice for allowing a maximum deformation rate of 2 mm per year. The deformation rate, and therefore the number of iterations needed to reach convergence, depends on the length of the chosen timestep and on the chosen rheology of the Earth's mantle. The length of the timestep must not be too short to provide a long computation time but a long timestep might not fulfill the convergence criteria. Tests are done using different rheologies to investigate the optimal length of the timestep.

It is assumed that the Earth is in isostatic equilibrium at the start of the simulation. Therefore, the iterative process starts at 120,000 years before present and runs forward till present day, starting with the ice-sheet-shelf model. Since the deformation is unknown for each timestep and the ice-sheet-shelf model requires the deformation, an initial guess for deformation must be done. The final deformation from the last timestep is chosen as initial deformation for the new timestep. For this reason, the length of the timestep must be chosen carefully.

A timestep of 5000 years is chosen from 120,000 years till 10,000 years BP for three reasons. The rate of deformation does not vary significantly over 5000 year in the first 100,000 years of the simulation and thus fulfills the assumption for the initial guess at each timestep, the deformation converges for the chosen convergence criterium and the computation time for one timestep is realistic. However, similar deformation rates cannot be assumed shortly before and after LGM, therefore a coupling timestep of 1000 years is chosen for the period from 20,000 years

BP till present day. The number of iterations that is needed to fulfill the convergence criterium is highly dependent on the chosen viscosity but is mostly between the 3 and 6 iterations.

The developed method is applied on a GIA FEM model and the ice-sheet-shelf model ANICE. The forward modelling approach required major adjustments of the GIA model. Also, ANICE required adjustments to include the deformation and to compute the grounded ice and ocean load. The load input for the GIA model must be defined on an equidistant grid using an Asia centered global projection with a resolution of 0.25 degrees latitude and longitude. The grid of ANICE is a polar centered grid for Antarctica with a resolution of 40 by 40 kilometers. Therefore, interpolation between the models is needed to couple the models.

Linear interpolation, Green's function and the quadrant method are tested for interpolation from ANICE to the FEM model. Linear interpolation, Green's function and the radius method are tested for interpolation from the FEM model to ANICE. The quadrant method and the radius method are performed using Oblimap and provide the most detailed results. A great advantage is the fast computation time of Oblimap of only a few seconds. Oblimap is integrated in the coupled model to perform the interpolation. The final result is a new method to simulate the interaction between GIA and ice sheet dynamics and a fully coupled ice dynamic-3D GIA model with coupling timesteps of 5000 and 1000 years.

*What is the accuracy of the method?*

Since the iterations do not perfectly convergence to zero, an uncertainty is introduced at every timestep. The uncertainty accumulates over time, revealing certain regions where the deformation rate is too high or the mantle viscosity too low to reach convergence to zero at every timestep. The uncertainty of the convergence method in the first 100 000 years is concentrated to four regions: the Weddell sea embayment, the Ross sea embayment and, to a lesser extent, the peninsula, and the Lambert Ice Shelf in East Antarctica. The cumulative uncertainty at modern date goes up to 8 mm per year for certain areas of the Ross Ice Shelf and the Ronne Ice Shelf and several ice shelves of the East Antarctic Ice Sheet. Considering the higher deformation rates at these regions, the accumulated uncertainty is acceptable but not neglectable. The regions where the change in ice thickness is high are more reactive to the GIA feedback effect. Furthermore, the uncertainty of the deformation rate does never exceed 1 mm per year per timestep for the tested rheologies, which is relatively low compared to the time averaged deformation rate itself of up to 30 mm per year.

Increasing the number of iterations by decreasing the convergence criterium of 2 mm deformation per year will lead to a smaller range of elements that alternate between a positive and negative value. It also decreases the range of deformation itself. However, convergence to zero cannot be reached solely by decreasing the convergence criterium. Decreasing the timestep or using relatively high viscosity values for the upper mantle does decrease the required number of iterations to reach convergence. This also decreases the area that does not convergence to zero, and thus decreases the uncertainty.

*What are the differences in ice sheet thickness, grounding line position and deformation when using a laterally varying Earth structure compared to a laterally homogeneous Earth structure for the Antarctic Ice sheet?*

The importance of the effect of using a 3D rheology to simulate the ice sheet evolution depends on the rheological model that is used. A higher water content, smaller grain size and higher temperatures in the upper mantle lead to increasing deformation rates. The deformation rate increases at the Antarctic Peninsula, the Ronne Ice Shelf and the west side of the Ross Ice Shelf from maximum 20 mm per year to maximum 30 mm per year when using the 3D wet rheology instead of the 1D rheology. There are locations in East Antarctica where the deformation doubles from approximately 10 mm per year to 20 mm per year.

It follows from the results that the increasing deformation rates lead to increasing changes in ice thickness for both 3D rheologies when compared to ice thickness using a 1D rheology. A change in ice thickness impedes changes in the grounding line migration as well. At most locations, the calving and grounding line do not change more than 20 kilometers when using different 1D and 3D rheologies. However, local grounding line position variances of more than 20 kilometers do exist. The grounding line difference between the 1D rheology and 3D wet rheology can go up to 200 kilometers at locations where the difference in ice thickness is 100 meters or more, such as the Ross Ice Shelf and the Ronne Ice Shelf. The deformation pattern is similar when using three different rheologies, but the magnitude differs. The results of this study emphasize the importance of using a realistic range of rheologies for the analyses of the local ice sheet evolution.

*What is the effect of the interaction between Glacial Isostatic Adjustment and ice sheet dynamics on the Antarctic Ice Sheet growth during the last glacial cycle?*

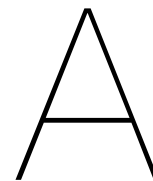
By developing the coupled model, research can be performed on the effect of GIA feedbacks on ice dynamic characteristics over the past 120 000 years for the AIS. The first timestep, 120,000 to 115,000 BP, is analyzed in detail using a 1D rheology and two different 3D rheologies. The maximum difference between the uncoupled deformation (iteration 1) and the coupled deformation (average between the last two iterations) for the period 120,000 to 115,000 years BP is 3 to 8 mm per year, depending on the viscosity of the upper mantle. The maximum difference in ice thickness at 115,000 years BP is 50 meters close to the Ronne Ice Shelf and the Ross Ice Shelf. The grounding line position differs up to 80 meters when applying the coupling method compared to the uncoupled result.

The GIA feedback effect enhances deformation and ice dynamic processes at high elevations in East Antarctica and around fast flowing ice sheets like the Ronne Ice Shelf, the Ross Ice Shelf, and the Amery Ice Shelf. The GIA feedback effect weakens the deformation signal at the embayment's of the Bellinghousen, Lazarev, Riiser-Larsen, and Mawson seas.

By knowing the effect of GIA feedback on local ice dynamics, better uncertainty estimates can be made for ice models that do not include the GIA feedback effects and for ice models that use prescribed ice loading. The coupled model contributes to a more precise simulation of the evolution of the AIS and to better estimates of the present-day ice sheet characteristics and GIA effect. Better estimates for GIA and ice sheet characteristics will lead to a more precise correction for ongoing GIA to modern geodetic data and to better calibration of forecasting models. Ultimately, these new insights will help to estimate the effect that climate change will have on the lives of flora, fauna, and people worldwide.







## Ice dynamic model

ANICE is a dynamic ice model that can simulate the evolution of the ice sheet at 4 regions Greenland, Eurasia, North America and Antarctica separately. For the coupled model, ANICE only simulates the Antarctic region. The change in ice height over time is dependent on the horizontal velocity profile over the whole height of the ice and the mass balance of the ice sheet. The mass increase through precipitation and refreezing and decrease through ablation and basal melt.

The growth and decay of the ice sheet is driven externally forced the atmospheric temperature and the sea level. The global eustatic sea level and atmospheric temperature that are used to force ANICE are shown in Figure S.1 in the supplementary materials. ANICE does not include the Sea Level equation so a mean sea level is applied everywhere. Therefore, self-gravitation of the ice sheet is not considered and regionally the sea level will be higher where the ice mass is bigger and lower than the mean where the ice is thinner. This effect can be several tens of meter but is much smaller during last glacial maximum to present due to fast melting. The bedrock deforms due to this change in load as well, but this is a second order effect.

As described in section 2.1 of the article, ANICE uses the SSA (Bueler and Brown, 2009) to solve mechanical equations for ice shelf dynamics and the SIA to solve for grounded ice (Morland, 1987; Morland & Johnson, 1980). Shear stresses are a result of the vertical differences in horizontal velocity. The SIA assumes that the horizontal shear stress is large with respect to normal and longitudinal stresses and that there is no basal sliding leading to less melt at the base of the sheet due to reduction of friction.

The SSA assumes larger longitudinal stresses with respect to horizontal shear stress. The subwater system in West Antarctica leads to a lower friction because of erosion and melt, although is not fully incorporated in ANICE (Fricker et al., 2007). A grid point is modelled as a fluid where gravity causes spreading.

### A.1 Forcing

Precipitation is dependent on the amount of water vapor in the atmosphere and melt on the top of the ice sheet depends on radiation and temperature of the atmosphere. Precipitation is defined monthly and increases during wintertime from March to September, especially at the Southern Ocean around East Antarctica and south of the peninsula. Precipitation over the East Antarctic ice sheet is approximately zero through all seasons.

The surface temperature over the East Antarctic ice sheet is much colder during March till October and goes down to -60 degrees Celsius compared to approximately -20 during November till February. The surface temperature at the Antarctic peninsula is more stable over the year and

decreases to approximately -30 degrees Celsius during winter months, compared to 0 to -10 degrees Celsius in summertime.

A few assumptions have been done for initial values at 120,000 years BP. It is assumed that the bedrock topography, grounded ice thickness and the surface elevation are the same as they are at present day. It is assumed that the ice sheet was in equilibrium at the start of the simulation so vertical and horizontal velocities and bottom melt were zero.

## A.2 Including the calculated GIA file in ANICE

In earlier versions of ANICE, GIA is included using the SELEN method by de Boer et al. (2017) or the ELRA method by Oude Egbrink (2017). The use of these methods can easily be switched off by an option in the configuration file. The file *ant\_grice\_module.f90* contains the main routine for the simulation. The routine is modified to read a file that contains the deformation over the full timestep, which is the output from the GIA model. In the original model used by Oude Egbrink (2017), the bedrock height at the end of the timestep was calculated using the ELRA method. In the coupled model, the bedrock height is calculated by adding the change in bedrock height to the initial bedrock height of the timestep. The new bedrock height is calculated using Equations A.1 and A.2.

$$\text{Bedrock height per year} = \frac{\text{Deformation}}{\text{Total time of timestep}} \quad \text{A.1}$$

$$\begin{aligned} \text{Bedrock height new} \\ = \text{Bedrock height} + \text{Bedrock height per year} \cdot \text{dynamic timestep} \end{aligned} \quad \text{A.2}$$

It is important that the option *dt\_bedrock\_config* in the file *Config\_file\_ant* is set equal to the timestep chosen in the GIA model because the deformation is divided by the timestep to compute deformation rates per year.

The *restart\_file* is an output of ANICE and is written at the beginning and end of the timestep. This file contains important variables that are needed for the next timestep like bedrock height and ice thickness.

The grid of ANICE is a polar centered grid and the GIA model a global equidistant grid. Interpolation is done to calculate deformation on the ANICE grid (see Appendix C).

# B

## GIA model

Two different approaches are used in literature to define a GIA model, the Finite Volume Method (FVM) and the Finite Element Method (FEM). An FVM model computes deformation on the center of cell (Figure B.1b). This allows for a higher spatial resolution (up to 6 km near the surface and 50 km below 350 km depth) and solves the deformation effectively on an irregular grid (Gomez, 2018). However, this method is computationally very expensive. The parametrization of an Earth model using a commercial FEM was developed by Wu (2004). A FEM model computes deformation at the nodes of an element (Figure B.1a). This is computationally more effective than the finite volume approach. The finite element model approach is chosen for the GIA model used in this study because it is relatively easy to develop using ABAQUS and it is possible to adjust the resolution at the area of interest.

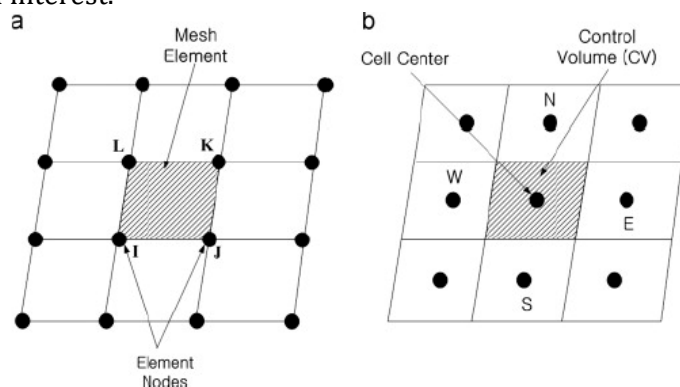


Figure B.1: Difference between finite volume approach and finite element approach (Latychev et al., 2005).

### B.1 Generation of a layered model

First, the spherical model of the Earth is generated by *Model\_gen.py* using *model\_data.py*. *Model\_data.py* contains the input settings and the time vector is defined here. The output is the ABAQUS model database *Earth.cae*. In the original model, this module generates the model with a certain grid and applies the load since the ice load is pre-known (Blank et al., in prep). The model developed for this study uses the same module to generate the model but since the load is unknown, the code is modified so that the load is applied in the module *Iter\_ult.py* instead of *Model\_gen.py*.

### B.1.1 Generate inner and outer core, lower mantle and crust

The inner and outer core are defined as one layer at depth 2891 to 6371 kilometers. The core is assumed to consist of incompressible isotropic elastic material. However, Abaqus cannot simulate with fully incompressible materials so a Poisson ratio of 0.4999 is used instead of 0.5. The mantle is divided in 4 layers. The lower mantle consists of two layers at depth 670 to 1171 kilometers and 1171 to 2891 kilometers and consisting of the same material properties. The crust is defined by one layer at depth 0 to 70 kilometers. The properties for the material in the core and the lower mantle are shown in table B.1.

Table B.1: Material properties of the core, the lower mantle, and the crust.

	Density [kg/m <sup>3</sup> ]	Young modulus [Pa]	Shear modulus [Pa]	Poisson ratio [-]	Viscosity [Pa*s]
Core	10750	3-20	1 <sup>-20</sup>	0.49	0
Lower mantle	4978	3-20	2.28340 <sup>1</sup>	0.49	2·10 <sup>21</sup>
Asthenosphere & upper mantle	4978	3-20	2.28340 <sup>1</sup>	0.49	Variable
Crust	3037	0.5060	0.50605 <sup>1</sup>	0.49	1 · 10 <sup>44</sup>

### B.1.2 Upper mantle & Asthenosphere

The upper mantle and the asthenosphere are defined as two layers at depth 70 to 420 kilometers and 420 to 670 kilometers respectively. The properties for these two layers are equal and shown in table B.1. The viscosity of these layers has a big influence on the deformation of the Earth's surface and therefore varies per simulation to test this influence, as explained in section 2 of the article. When using a 3D Earth structure, the material of the upper mantle and the asthenosphere is set to creep and a user\_f routine is used to read in the creep parameters.

Deformation takes place via 2 processes, diffusion and dislocation creep, as explained in section 1. The computation of the viscosity using creep parameters is based on the approach of van der Wal et al. (2013). Diffusion creep is mainly dependent on grain size and is the deformation process for higher temperatures, high water content and a small grain size. Diffusion is linearly dependent on stress and largely dependent on grain size. Dislocation is caused by stress and is mainly dependent on the water content. When a high load is applied, dislocation is the main process of material movement. Dislocation is linearly dependent on grain size but nonlinearly dependent on stress. When the load is smaller, diffusion takes over.

Dislocation and diffusion parameters are derived by using seismic models which is described in section 2 of the article. To assign the viscosity to an individual element in the FEM model, the following definition of effective viscosity is used (van der wal, 2013):

$$\eta = \frac{1}{3 \cdot B_{diff} + 3 \cdot B_{dist} \cdot q^{n-1}} \quad \text{B.1}$$

Where  $q$  is the von Mises stress and  $n = 3.5$ . From the creep parameters, the *User\_2.f* subroutine calculates the strain. Abaqus uses the calculated strain from de user subroutine as input.

### B.1.3 Assembly and mesh

Each layer is divided in a grid. The resolution of the grid at the surface is approximately 200 by 200 kilometers, but can easily be upscaled to 55 km and radially 70 km at the Antarctic region. The input is given on an equidistant grid of  $\frac{1}{4}$  of 1 degree latitude and longitude. 1 degree is approximately 100 kilometers in latitude direction so the resolution is approximately 25 kilometers, dependent on the distant to the south pole. There is a tie build between each layer in Abaqus so stress can be transferred from one layer to the other. If there is a density difference between layer, the winkler foundation is applied to model the buoyancy stress. If the density between layers is equal, the buoyancy is zero.

Element types are set to hybrid. Hybrid elements have an extra degree of freedom to approach incompressibility of the material, which is a main limitation of the approach of Wu (2004).

## B.2 Input: define ice and ocean loads

Ice and ocean load are applied on the model with respect to the initial timestep. Ocean water has a density of 1000 kg/m<sup>3</sup> and the density of ice is assumed to be 920 kg/m<sup>3</sup>. The load applied on the FEM model is calculated by multiplying the thickness of the layer of ice or ocean with the density and the gravitational acceleration of 9.81 m/s<sup>2</sup>. The load is applied linearly over time per timestep using the ramp load option in ABAQUS.

The relative sea level corresponds to the geoid minus the change in thickness of the water column. As described in section 2.2 of the article, the relative sea level is calculated using Whitehouse et al. (2012), Schaeffer and Lebedev (2013), and Heeszel et al. (2016). However, the the relative sea level is computed for the period 110,000 years BP to modern date. Linear interpolation is used to calculate the relative sea level at each timestep chosen for this study, where conservation of mass is taken into account. At each timestep, the global relative sea level is multiplied with a land-mask for Antarctica to exclude elements that are land.

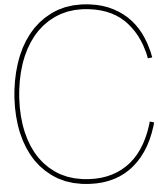
## B.3 Running the FEM model

Spherical harmonics 0 and 1 are deleted from the ice and ocean load. Several tests are done to determine the variation of spherical harmonics 0 and 1 when computing the spherical harmonics with different maximum degrees. Spherical harmonics 0 and 1 are barely changing when increasing the maximum calculated degrees so a degree of 5 is chosen. The deformation at each grid point is computed by the routine *Iter\_ult.py*.

The iterations follow the routing from Wu et al. (2004) using the subroutine *sph\_tools.py* to account for self-gravitation of the Earth. In *sph\_tools.py*, again the spherical harmonics 0 and 1 are removed but this time the spherical harmonics are calculated till degree 90 because of the much higher influence on spherical harmonics 0 and 1.

Every timestep, the deformation is calculated using the file "Iter\_ult.py". At every grid point, the load is applied to the model and the deformation is calculated taking into consideration the

material properties of that grid point and the layers below till the center of the Earth. The deformation causes another deformation because of the self-gravitating effect. Therefore the deformation is calculated in a second iteration. In order to save computing time, the original model calculates the first iteration of every timestep and then calculates the second iteration. However, this concept cannot be used in the coupling method because the ice thickness for the next step is unknown. Therefore, the new model is rebuilt using a restart concept by Weerdesteijn (2019).



# Interpolation between model grids

The GIA model is defined on an equidistant grid using an Asia centered global projection with a resolution of 200 by 200 kilometers. The grid from ANICE is a polar centered grid for Antarctica with a resolution of 40 by 40 kilometers. Therefore, interpolation between the models is needed to couple the models. This appendix describes the influence of different interpolation methods.

## C.1 Interpolation ANICE to FEM

Linear interpolation is a fast method to interpolate data. In this case, the geodetic coordinates specified by the latitudes and longitudes of the original grid (the ellipsoidal height is assumed to be zero) are transformed to the geocentric Earth-Centered Earth-Fixed Cartesian coordinates specified by X, Y, and Z. The reference spheroid for the geodetic coordinates is assumed to be WGS84 Ellipsoid. The original data is linearly interpolated to the new grid, which is a mesh grid specified by X, Y and Z (the radius of the sphere is assumed to be 6371 km). The minimum curvature spline solution provides re sampled data on a regular grid. The solution can be constructed as a sum of contributions from each data point, weighted by Green's function evaluated for each point. Surface gradients can be used as data constraints. A MATLAB script written by Wessel and Becker (2008) is used to apply Green's function method for a spherical surface spline. In case the constraining data are noisy or do not reflect a smooth phenomenon, unwanted oscillations in the solution can occur. Introducing tension can counteract the tendency of splines to oscillate away from data constraints. However, introducing tension increases the computation time significantly.

For four different regions, North America, Eurasia, Greenland and Antarctica, ice thickness on a 20 km grid resolution is the output of the ice model. This is interpolated to a coarser grid of the Earth model, with a resolution of a quarter of a degree using the linear method, Greens method

and the quadrant method. Since the ice model provides output of four separate regions, these regions are first separately interpolated to the coarse grid and consecutively summed up.

To determine the best interpolation method in terms of detail and calculation time, the ice thickness output of 20 000 years before present of the ANICE model is chosen as the example. The ice thickness output of Antarctica can be seen in Figure C.1. The interpolated results of the linear method, Greens method and quadrant method can be seen in figures C.2, C.3 and C.4 respectively. Linear interpolation results in a significant loss of detail as well as a decrease in maximum ice thickness with 1 kilometer. Greens method provides a detailed result of the data but oscillations can be seen. Introducing tension could prevent oscillations. However, this method is highly time consuming, especially when tension is introduced. This will delay the coupled model significantly. The quadrant method provides a very detailed result and the calculation

takes several seconds using Oblimap. Therefore Oblimap is chosen as the preferred method to couple the Earth and the ice model.

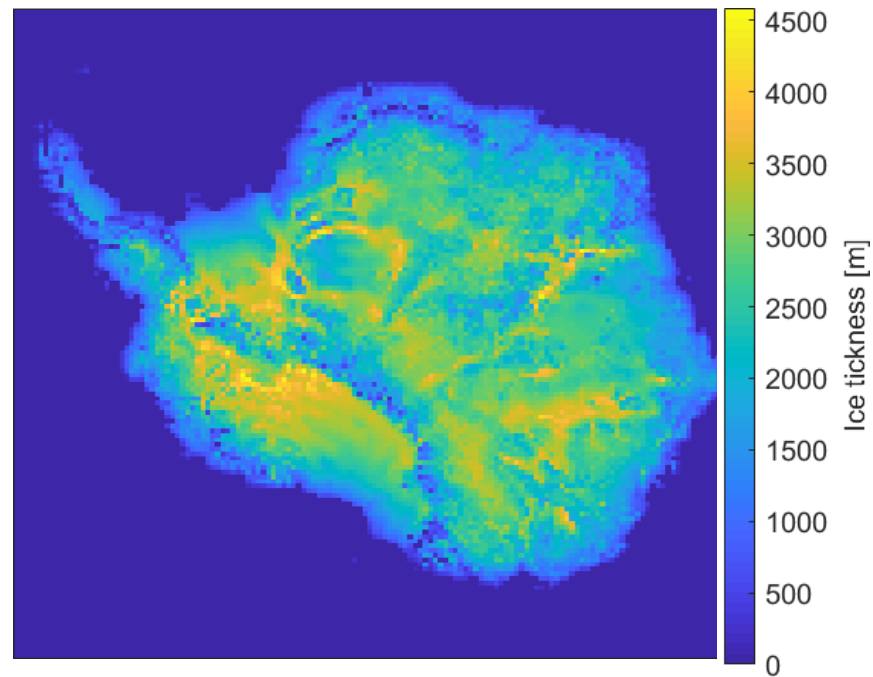


Figure C.1: Ice thickness at Antarctica. Output from the ANICE model at a polar centered grid.

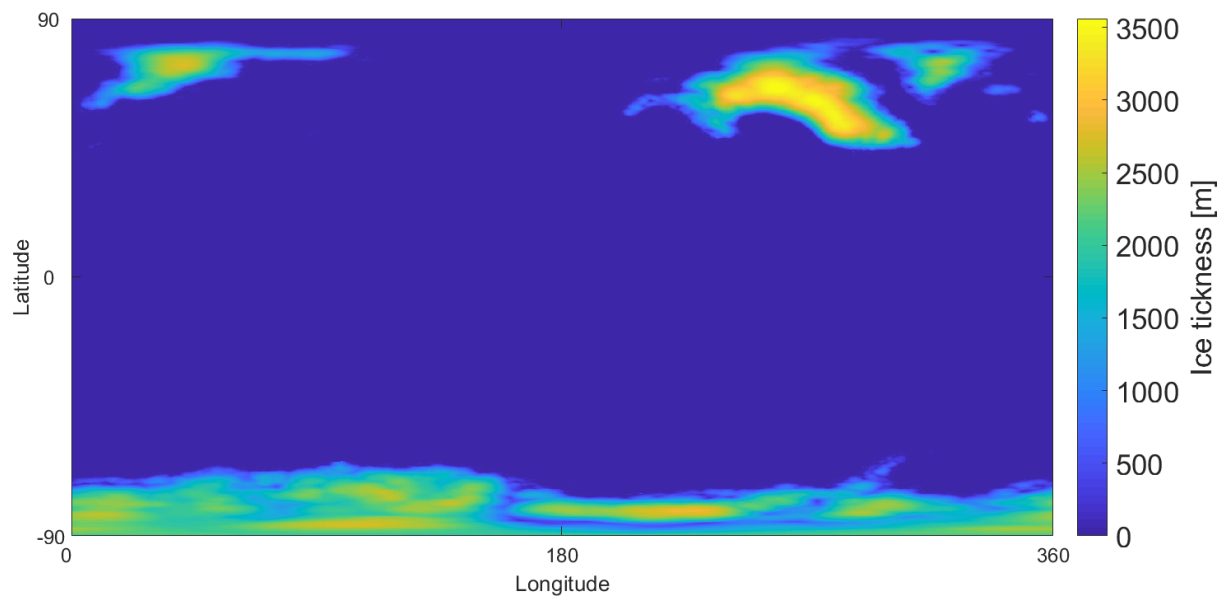


Figure C.2 Ice thickness at all longitudes and latitudes at a resolution of a quarter of a degree, linearly interpolated.



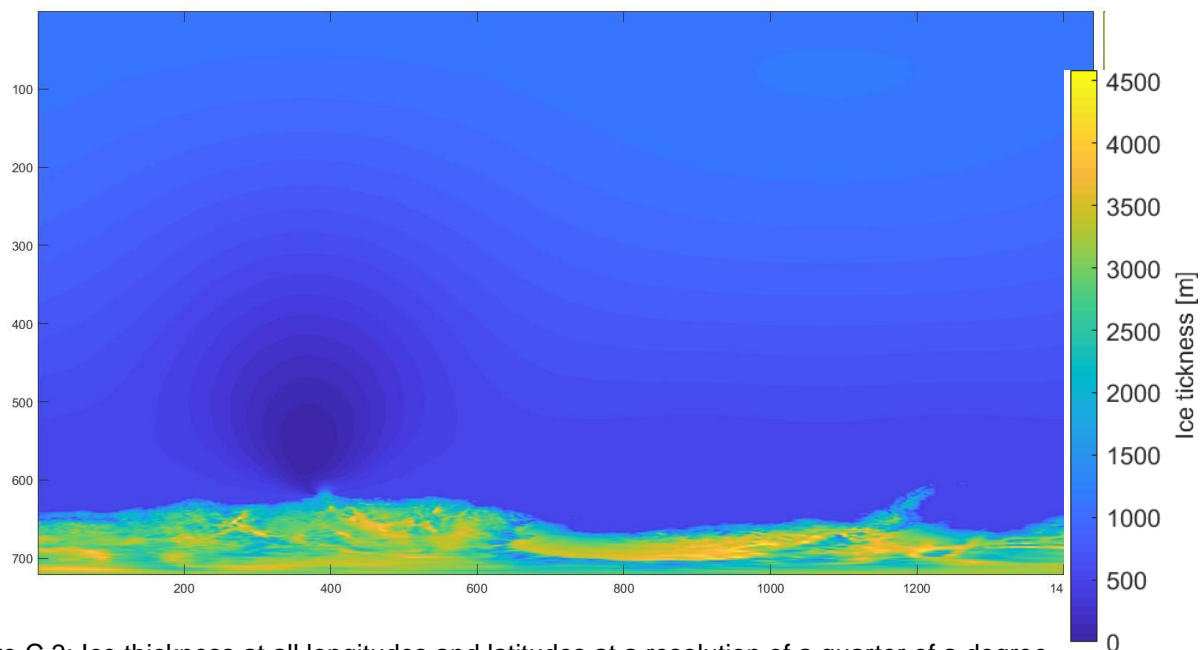


Figure C.3: Ice thickness at all longitudes and latitudes at a resolution of a quarter of a degree, interpolated using Greens method. No plane tension is apparent, sinusoides are visible.

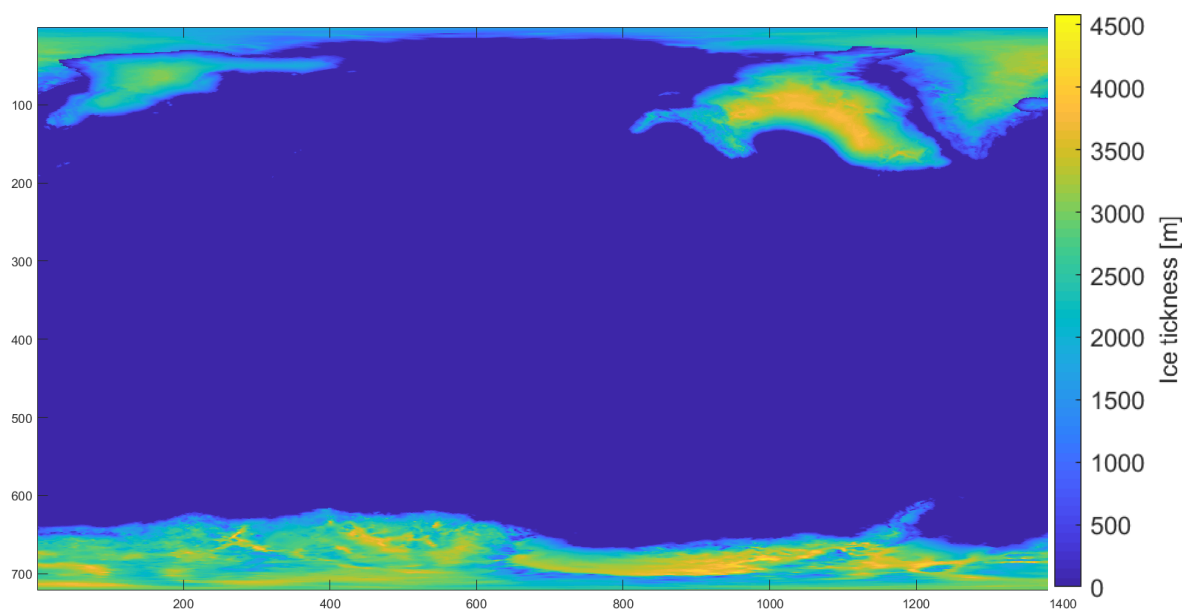


Figure C. 4: Ice thickness at all longitudes and latitudes at a resolution of a quarter of a degree, interpolated using quadrant method. Note that the ice sheet are not integrated with each other in this version of Oblimap. This problem is addressed in the final version that is used for the simulations.

## C.2 Interpolation FEM to ANICE

The deformation of the Earth's surface is calculated on a irregular relatively coarse grid whereas the ice thickness is calculated on a regular relatively fine grid. To use the deformation output of the Earth model as input for the ice model and the ice thickness output of the ice model as input for the Earth model, the data must be interpolated. The output of the Earth model is the deformation of the Earth's surface on a grid with a resolution of a quarter of a degree for a longitudes and latitudes. Since the ice model will only simulate Antarctica in the coupled model, the interpolation to the finer ice model grid is only been done for the region Antarctica.

Four gridding methods are considered: linear interpolation, Green's function method for a spherical surface spline, quadrant method and radius method. To choose the best interpolation method, the deformation output at time 20 000 years before present, with input from the ice model w12 is used to test the interpolation methods (Figure C.5). The deformation is interpolated with the linear method and the radius method, this can be seen in figures C.6 and C.7 respectively. The radius method provides a more detailed result and it can be calculated in several seconds using Oblimap, therefore the radius method is chosen as the preferred method to couple the Earth and the ice model.

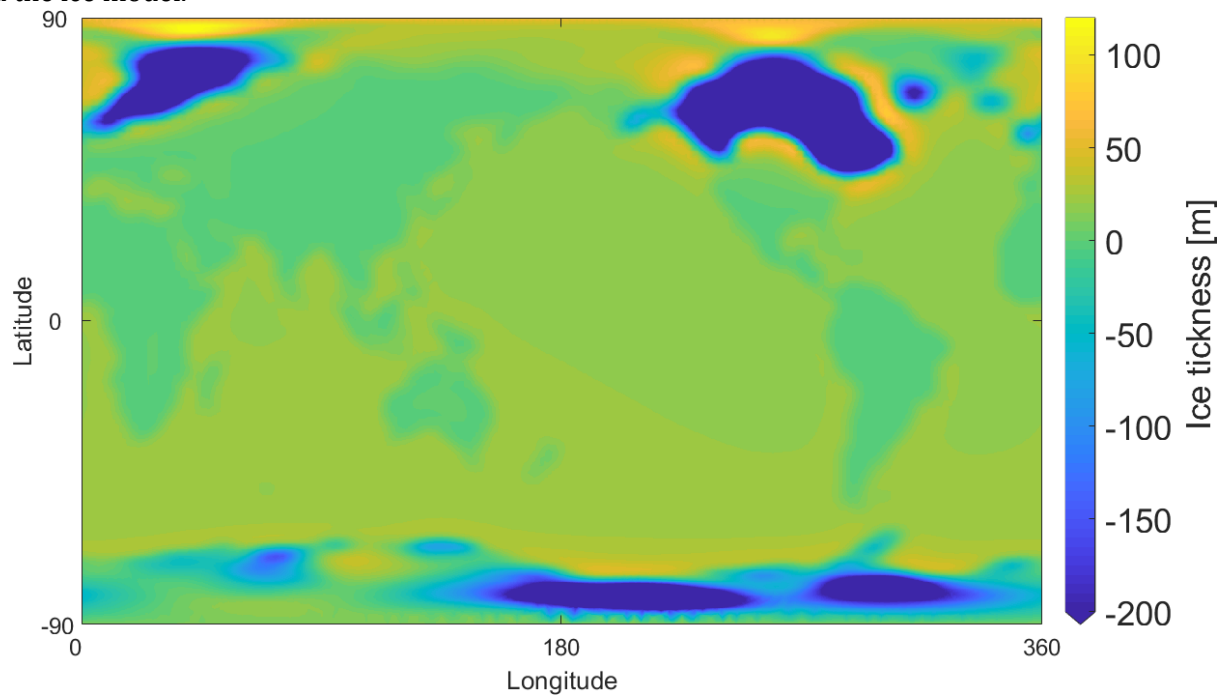


Figure C.5: Deformation of the Earth's surface from 120 000 till 20 000 years before present.

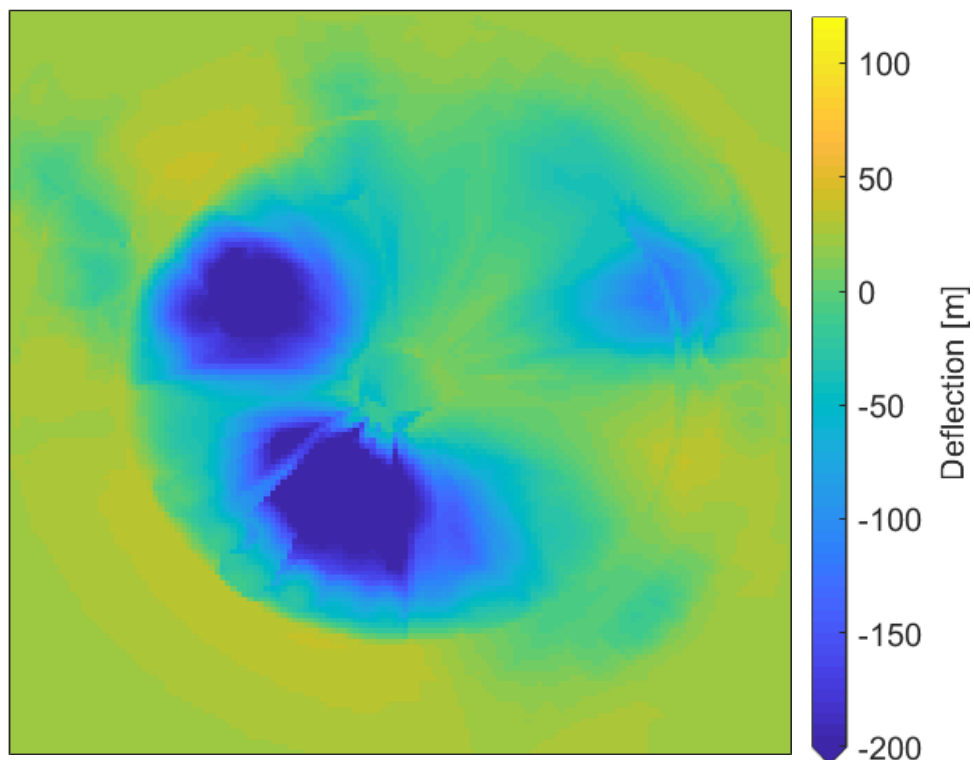


Figure C.6: Deformation of Antarctica interpolated to a polarcentered grid using the linear method

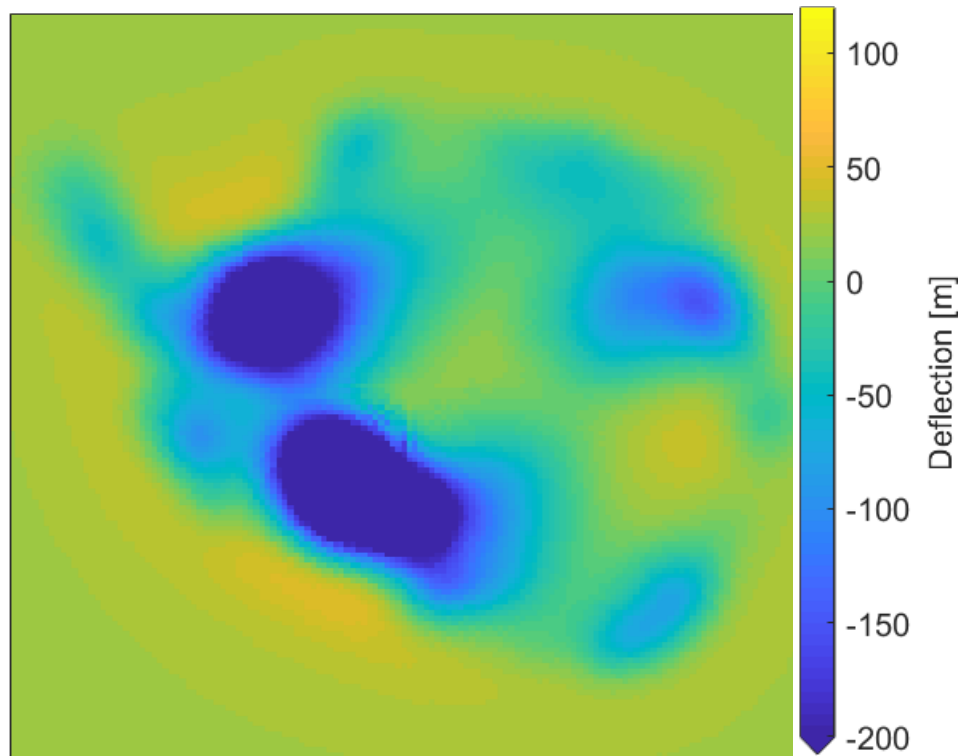


Figure C.7: Deformation of Antarctica interpolated to a polar centered grid using the radius method.





## Method

### D.1 Conversion of the model

Two different conversion criteria are tested and evaluated. First, the change in total grounded ice thickness should be smaller than 1 meter. However, when there is fast melting or growing of ice during the timestep, ice thickness is varying a lot. Especially around the grounding line. If ice thickness builds up more than 120 meters at the grounding line, the ice will calve and become an iceberg or an ice shelf. Depending on the deformation of the Earth's surface, ice can be grounded in one iteration and floating in the next iteration.

From the tests of these two criteria, it can be concluded that deformation and ice thickness converge to zero in most places but do not converge to zero at varying places around the grounding line where ice thickness change is high. At these places, the deformation and ice thickness will converge to a bigger range, dependent on the change of the ice thickness. Therefore, the last criterium is chosen to determine conversion and calculated with formula's D.1 and D.2.

$$\text{Difference}_1 = \text{Deformation}_j - \text{Deformation}_{j-1} \quad \text{D.1}$$

$$\text{Difference}_2 = \text{Deformation}_{j+1} + \text{Deformation}_j \quad \text{D.2}$$

Convergence has been reached if the condition in formula D.3 has been met at each grid point.

$$| \text{Difference}_1 + \text{Difference}_2 | \leq 2 \quad \text{D.3}$$

The converted ice thickness and deformation lies in between  $\text{Deformation}_j$  and  $\text{Deformation}_{j+1}$ . Therefore, the mean is calculated at every grid point and chosen as the converted ice thickness and deformation.

A characteristic timestep for GIA is 5000 years. In West Antarctica, the relaxation time is about tens or 100 years. Tests have been performed using a timestep of 1000, 2500 and 5000 years for the period 115,000 to 110,000 years BP. The uncertainty range is growing per timestep, but it still converges. The more change in ice thickness, the higher the uncertainty range. The error is not necessarily growing bigger with time because the elements that do not converge to zero change per timestep because of a different ice growth. However, the regions that do not convergence to zero always lie around the grounding line. A timestep of 5000 years has been chosen as the timestep but a different viscosity profile might need a different timestep.

## D.2 Recommendations for model improvement

The computation of deformation and ice dynamics by the FEM model and ANICE are done using dynamic time intervals to include nonlinearities. Due to time constraints, these nuances in changes over time are not included in the coupled model. The mean deformation and change in ice mass are computed over time and applied linearly on the model. This causes an underestimation of the deformation at the start of the timestep in the GIA model (Barletta et al., 2018).

The grid used by the GIA model is coarser than the grid used by ANICE. However, the input file for the GIA model that contains the load is on a finer grid than ANICE. The input data is then interpolated to the GIA grid using Abaqus. This causes unnecessary interpolation errors and could be solved by interpolating from the ANICE grid directly to the coordinates of the GIA grid. The same accounts for the deformation file. Deformation is computed on the model grid, interpolated to an output grid and then interpolated to the ANICE grid. One interpolation step could be avoided by interpolating directly from the model grid to the ANICE grid.

One of the solutions to increase computational speed is to include less iterations within each timestep. Research should be done into the performance of the model when using less iterations. A dynamic amount of iterations could be implemented, dependent on ice thickness change. The higher the change in ice thickness, the more iterations should be done.

The model is not tested for the effect of the initial topography (BEDMAP2). Although the computed bedrock topography at present day is similar to the BEDMAP2 topography, the effect of a different initial topography is unknown. Recently, a new bedrock topography is developed by Morlighem et al. (2020). This topography could be used to test the sensitivity of the model to the initial topography.

Since the coupled model is highly computational expensive and time consuming, it would be interesting to compare the coupling method to ANICE using the ELRA model to weigh up computation and time expensive factors to improvement of the results. A method developed by Oude Egbrink (2018) could be used calculate the relaxation time that coincides with the viscosity used in the 1D coupled model.

The last timestep to calculate present day rates is 1000 years. This is not representative for the present day deformation rate. Therefore, an additional timestep of 10 years after present day should be simulated to compute present day deformation and ice decay rates.

For this study, the assumption has been made that the Poisson ratio of the different layers is 0.49 to approach compressibility, which is assumed by the method of Wu (2004). However, a value of 0.28 would be closer to the observed Poisson ratio. Therefore, testing with this Poisson ratio could lead to improved results.